Chapter 1
Introduction

1.1 What Is $k \cdot p$ Theory?

Bir and Pikus [1] made the interesting observation, since the physics of semiconductors is (for the most part) governed by the carriers in the extrema of the various energy bands, that: first, only the neighborhoods of the band extrema are important and, second, the qualitative physics should be governed by the shape of these energy surfaces – a property that should be readily obtainable from symmetry arguments. The first observation has led to the common view of $k \cdot p$ theory as a perturbative theory as explified by the seminal work of Dresselhaus et al. [2] and Kane [3], while the second one has manifested itself through the power of symmetry analysis such as the method of invariants introduced by Luttinger [4].

The fact that one can go beyond the neighborhood of band extrema (by not using perturbation theory) was already demonstrated by Cardona and Pollak in 1966 [5], when they obtained realistic band structures for Si and Ge using a full-zone $k \cdot p$ theory. Thus, $k \cdot p$ theory is an empirical band-structure method with a basis of band states. This definition can be extended to nonperiodic systems such as impurities [6] and nanostructures [7] by replacing the Bloch phase factor by an envelope function.

1.2 Electronic Properties of Semiconductors

The subtitle of the book is the electronic properties of semiconductors. Specifically, we will show how the $k \cdot p$ method can be used to obtain the band structure of four types of semiconductors: those with a diamond, a zincblende, and a wurtzite structure, and of their nanostructures (Fig. 1.1). For those not familiar with their band structures, we hereby present a very brief description.

Diamond and zincblende are closely related and they will, therefore, be discussed together. They both have cubic symmetry with two atoms per primitive unit cell (see Appendix B for details). They are mostly the group-IV elements such as Si, the III-V compounds such as GaAs, and a few II-VI compounds such as CdTe. Most of them are direct-gap semiconductors, though some are indirect (e.g., Si and GaP)

L.C. Lew Yan Voon, M. Willatzen, *The* k · p *Method*,
DOI 10.1007/978-3-540-92872-0_1, © Springer-Verlag Berlin Heidelberg 2009

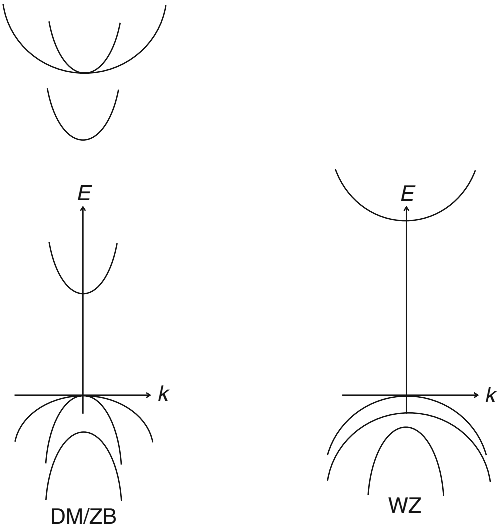

Fig. 1.1 Band structures to be studied in this book: diamond (DM), zincblende (ZB), wurtzite (WZ), and their nanostructures

and others are semimetallic (e.g., Sn [8] and HgTe [9] have a negative gap). For the semiconductors, the band gap tends to separate a valence band derived from atomic-like *p* orbitals and a conduction band derived from atomic-like *s* orbitals. The maximum of the valence band is, for most materials, at the zone center of the Brillouin zone ($\mathbf{k} = \mathbf{0}$). In the absence of spin-orbit coupling and spin degeneracy, the highest valence band is, therefore, three-fold degenerate while the lowest conduction band is nondegenerate. With spin-orbit coupling, the valence band consists of a four-fold degenerate band at the zone center (though the degeneracy is reduced for finite wave vectors into either two two-fold degenerate bands—so-called light and heavy-hole bands—or further splittings into nondegenerate states due to the phenomenon of spin splitting for zincblende) and a two-fold spin-hole split (also known as spin-orbit split) band.

Wurtzite has a primitive unit cell with four atoms and is the stable structure for many of the II-VI compounds (e.g., ZnO) and a few of the III-V compounds (e.g., GaN). A useful picture of the wurtzite structure is to envision it as a zincblende one strained along the [111] direction. Hence, the band structure can also be derived from the zincblende case by adding a crystal-field splitting. The main consequence is that the six highest valence states of zincblende are mixed and split into three three-fold degenerate states at the zone center.

The above band pictures and their modifications in external fields and in nanostructures are what we will be describing in this book.

1.3 Other Books

This book is about the $k \cdot p$ method and the resulting electronic structure of semiconductor bulk and nanostructure. Our approach differs significantly from other recent books and review articles where some exposition of the $k \cdot p$ theory has been given but with the emphasis on the application to, e.g., modeling devices or interpreting various types of experiments. While bits of $k \cdot p$ theory can be found in most textbooks [7, 10–19], we now give a brief outline of some of the more advanced presentations of the $k \cdot p$ theory and how they differ from ours.

First, the only books that place a heavy emphasis on developing the $k \cdot p$ theory appear to be those by Bir and Pikus [1], Ivchenko and Pikus [20] and Winkler [21]. They are all very useful books in their own rights and would be worth consulting together with the current one. For example, the book by Bir and Pikus [1] was a milestone in that it finally provided the first compendium in English of the seminal research by russian physicists in using symmetry to develop the $k \cdot p$ theory, particularly in two areas not previously considered by Luttinger: the impact of deformations and the study of hexagonal crystals. The book by Ivchenko and Pikus [20] follows along the same lines but the focus is on applications to heterostructures and their optical properties. Taken together, they cover a lot of the $k \cdot p$ theory and its applications. However, the book by Bir and Pikus is a little bit dated while the one by Ivchenko and Pikus only devotes a chapter to explaining $k \cdot p$ theory. Furthermore, both books are currently out of print. The book by Winkler [21] is rather more focused and is probably the most comprehensive exposition of the spin-splitting theory. Zeiger and Pratt [12] give a very detailed discussion of the Luttinger–Kohn theory, particularly as applied to the magnetic problem. A significant part of the modern use of the $k \cdot p$ theory is applied to semiconductor heterostructures so it is not surprising that the newer books focus on such applications [7, 14, 15, 17–22].

In many ways, the current book is a combination of all of the above work (and of the work cited throughout, of course). Thus, we present a comprehensive and, for that reason, both a historical and modern exposition of the $k \cdot p$ theory for both bulk crystals and nanostructures, taking into account deformations, impurities, and external static electric and magnetic fields. One can also use this book as an aid to reading the original literature. Certainly, the book is aimed at people who wishes to learn how to derive $k \cdot p$ Hamiltonians.

Part I
Homogeneous Crystals

Chapter 2
One-Band Model

2.1 Overview

Much of the physics of the $k \cdot p$ theory is displayed by considering a single isolated band. Such a band is relevant to the conduction band of many semiconductors and can even be applied to the valence band under certain conditions. We will illustrate using a number of derivations for a bulk crystal.

2.2 $k \cdot p$ Equation

The $k \cdot p$ equation is obtained from the one-electron Schrödinger equation

$$H\psi_{n\mathbf{k}}(\mathbf{r}) = E_n(\mathbf{k})\psi_{n\mathbf{k}}(\mathbf{r}), \tag{2.1}$$

upon representing the Bloch functions in terms of a set of periodic functions:

$$\psi_{n\mathbf{k}}(\mathbf{r}) = \mathrm{e}^{\mathbf{i}\mathbf{k}\cdot\mathbf{r}}u_{n\mathbf{k}}(\mathbf{r}). \tag{2.2}$$

The Bloch and cellular functions satisfy the following set of properties:

$$\langle\psi_{n\mathbf{k}}|\psi_{n'\mathbf{k}'}\rangle \equiv \int \mathrm{d}V\, \psi^*_{n\mathbf{k}}(\mathbf{r})\,\psi_{n'\mathbf{k}'}(\mathbf{r}) = \delta_{nn'}\delta(\mathbf{k}-\mathbf{k}'), \tag{2.3}$$

$$\langle u_{n\mathbf{k}}|u_{n'\mathbf{k}}\rangle \equiv \int \mathrm{d}\Omega\, u^*_{n\mathbf{k}}u_{n'\mathbf{k}} = \delta_{nn'}\frac{\Omega}{(2\pi)^3}, \tag{2.4}$$

where V (Ω) is the crystal (unit-cell) volume.

Let the Hamiltonian only consists of the kinetic-energy operator, a local periodic crystal potential, and the spin-orbit interaction term:

$$H = \frac{p^2}{2m_0} + V(\mathbf{r}) + \frac{\hbar}{4m_0^2c^2}(\boldsymbol{\sigma}\times\nabla V)\cdot\mathbf{p}\,. \tag{2.5}$$

L.C. Lew Yan Voon, M. Willatzen, *The* k · p *Method*,
DOI 10.1007/978-3-540-92872-0_2, © Springer-Verlag Berlin Heidelberg 2009

Here, we only give the formal exact form for a periodic bulk crystal without external perturbations.

In terms of the cellular functions, Schrödinger's equation becomes

$$H(\mathbf{k})\,u_{n\mathbf{k}} = \mathcal{E}_n(\mathbf{k})\,u_{n\mathbf{k}}, \tag{2.6}$$

where

$$H(\mathbf{k}) \equiv H + H_{k\cdot p}, \tag{2.7}$$

$$H_{k\cdot p} = \frac{\hbar}{m_0}\mathbf{k}\cdot\boldsymbol{\pi}, \tag{2.8}$$

$$\boldsymbol{\pi} = \mathbf{p} + \frac{\hbar}{4m_0c^2}\left(\boldsymbol{\sigma}\times\nabla V\right), \tag{2.9}$$

$$\mathcal{E}_n(\mathbf{k}) = E_n(\mathbf{k}) - \frac{\hbar^2k^2}{2m_0}\,. \tag{2.10}$$

Equation (2.6) is the $k \cdot p$ equation. If the states $u_{n\mathbf{k}}$ form a complete set of periodic functions, then a representation of $H(\mathbf{k})$ in this basis is exact; i.e., diagonalization of the infinite matrix

$$\langle u_{n\mathbf{k}}|H(\mathbf{k})|u_{m\mathbf{k}}\rangle$$

leads to the dispersion relation throughout the whole Brillouin zone. Note, in particular, that the off-diagonal terms are only linear in k. However, practical implementations only solve the problem in a finite subspace. This leads to approximate dispersion relations and/or applicability for only a finite range of k values. For GaAs and AlAs, the range of validity is of the order of 10% of the first Brillouin zone [7].

An even more extreme case is to only consider one $u_{n\mathbf{k}}$ function. This is then known as the one-band or effective-mass (the latter terminology will become clear below) model. Such an approximation is good if, indeed, the semiconductor under study has a fairly isolated band—at least, again, for a finite region in k space. This is typically true of the conduction band of most III–V and II–VI semiconductors. In such cases, one also considers a region in k space near the band extremum. This is partly driven by the fact that this is the region most likely populated by charge carriers in thermal equilibrium and also by the fact that linear terms in the energy dispersion vanish, i.e.,

$$\frac{\partial E_n(\mathbf{k}_0)}{\partial k_i} = 0.$$

A detailed discussion of the symmetry constraints on the locations of these extremum points was provided by Bir and Pikus [1]. In the rest of this chapter, we will discuss how to obtain the energy dispersion relation and analyze a few properties of the resulting band.

2.3 Perturbation Theory

One can apply nondegenerate perturbation theory to the $k \cdot p$ equation, Eq. (2.6), for an isolated band. Given the solutions at $\mathbf{k} = \mathbf{0}$, one can find the solutions for finite k via perturbation theory:

$$E_n(\mathbf{k}) = E_n(\mathbf{0}) + \frac{\hbar^2 k^2}{2m_0} + \frac{\hbar \mathbf{k}}{m_0} \cdot \langle n\mathbf{0}|\boldsymbol{\pi}|n\mathbf{0}\rangle + \frac{\hbar^2}{m_0^2} \sum_l{}' \frac{|\langle n\mathbf{0}|\boldsymbol{\pi}|l\mathbf{0}\rangle \cdot \mathbf{k}|^2}{E_n(\mathbf{0}) - E_l(\mathbf{0})} \tag{2.11}$$

to second order and where

$$\langle n\mathbf{0}|\boldsymbol{\pi}|l\mathbf{0}\rangle = \frac{(2\pi)^3}{\Omega} \int \mathrm{d}\Omega \; u_{n\mathbf{0}}^* \boldsymbol{\pi} u_{l\mathbf{0}}. \tag{2.12}$$

This is the basic effective-mass equation.

2.4 Canonical Transformation

A second technique for deriving the effective-mass equation is by the use of the canonical transformation introduced by Luttinger and Kohn in 1955 [6]. Here, one expands the cellular function in terms of a complete set of periodic functions:

$$u_{n\mathbf{k}}(\mathbf{r}) = \sum_{n'} A_{nn'}(\mathbf{k})\, u_{n'\mathbf{0}}(\mathbf{r}). \tag{2.13}$$

Then the $k \cdot p$ equation, Eq. (2.6), becomes

$$\begin{aligned}\sum_{n'} A_{nn'}(\mathbf{k}) \left[H + H_{k\cdot p}\right] u_{n'\mathbf{0}}(\mathbf{r}) &= \sum_{n'} A_{nn'}(\mathbf{k}) \left[E_{n'}(\mathbf{0}) + H_{k\cdot p}\right] u_{n'\mathbf{0}}(\mathbf{r}) \\ &= \mathcal{E}_n(\mathbf{k}) \sum_{n'} A_{nn'}(\mathbf{k})\, u_{n'\mathbf{0}}(\mathbf{r}).\end{aligned} \tag{2.14}$$

Multiplying by $(2\pi)^3/\Omega \int_\Omega \mathrm{d}^3\mathbf{r}\, u_{n\mathbf{0}}^*$ gives

$$E_n(\mathbf{0})\, A_{nn} + \sum_{n'} \frac{\hbar \mathbf{k}}{m_0} \cdot \mathbf{p}_{nn'} A_{nn'}(\mathbf{k}) = \mathcal{E}_n(\mathbf{k})\, A_{nn}, \tag{2.15}$$

where

$$\mathbf{p}_{nn'} \equiv \mathbf{p}_{nn'}(\mathbf{0}) = \frac{(2\pi)^3}{\Omega} \int \mathrm{d}\Omega \; u_{n\mathbf{0}}^* \mathbf{p} u_{n'\mathbf{0}}, \tag{2.16}$$

and we have left out the spin-orbit contribution to the momentum operator for simplicity. Now one can write (dropping one band index)

$$H(\mathbf{k})A = \mathcal{E}(\mathbf{k})A, \quad A = \begin{pmatrix} \vdots \\ A_n \\ \vdots \end{pmatrix}. \tag{2.17}$$

The linear equations are coupled. The solution involves uncoupling them. This can be achieved by a canonical transformation:

$$A = TB, \tag{2.18}$$

where T is unitary (in order to preserve normalization). Then

$$\overline{H}(\mathbf{k})B = \mathcal{E}(\mathbf{k})B, \tag{2.19}$$

where

$$\overline{H}(\mathbf{k}) = T^{-1}HT. \tag{2.20}$$

Writing $T = \mathrm{e}^S, \quad T^{-1} = \mathrm{e}^{-S} = T^\dagger$,

$$\begin{aligned} \overline{H} &= \left(1 - S + \frac{1}{2!}S^2 - \cdots\right) H(\mathbf{k}) \left(1 + S + \frac{1}{2!}S^2 + \cdots\right) \\ &= H(\mathbf{k}) + [H(\mathbf{k}), S] + \frac{1}{2!}[[H(\mathbf{k}), S], S] + \cdots \\ &= H + H_{k\cdot p} + [H, S] + [H_{k\cdot p}, S] \\ &\quad + \frac{1}{2!}[[H, S], S] + \frac{1}{2!}\left[[H_{k\cdot p}, S], S\right] + \cdots \end{aligned} \tag{2.21}$$

Since $H_{k\cdot p}$ induces the coupling, one would like to remove it to order S by

$$H_{k\cdot p} + [H, S] = 0, \tag{2.22}$$

or, with $|n\rangle \equiv |u_{n\mathbf{0}}\rangle$,

$$\begin{aligned} \langle n|H_{k\cdot p}|n'\rangle + \sum_{n''}\left[\langle n|H|n''\rangle\langle n''|S|n'\rangle - \langle n|S|n''\rangle\langle n''|H|n'\rangle\right] &= 0, \\ \frac{\hbar}{m_0}\mathbf{k}\cdot\mathbf{p}_{nn'} + E_n(\mathbf{0})\langle n|S|n'\rangle - \langle n|S|n'\rangle E_{n'}(\mathbf{0}) &= 0, \end{aligned}$$

giving, for $n \neq n'$,

$$\langle n|S|n'\rangle = -\frac{\hbar}{m_0}\frac{\mathbf{k}\cdot\mathbf{p}_{nn'}}{[E_n(\mathbf{0}) - E_{n'}(\mathbf{0})]}. \tag{2.23}$$

Now, Eq. (2.21) becomes

$$\overline{H}(\mathbf{k}) = H + \frac{1}{2}[H_{k\cdot p}, S] + \frac{1}{2}[[H_{k\cdot p}, S], S] + \cdots$$

and, to second order,

$$\begin{aligned}\langle n|\,\overline{H}\,(\mathbf{k})|n'\rangle &\approx \langle n|H|n'\rangle + \frac{1}{2}\sum_{n''}\Big[\langle n|H_{k\cdot p}|n''\rangle\langle n''|S|n'\rangle - \langle n|S|n''\rangle\langle n''|H_{k\cdot p}|n'\rangle\Big]\\ &= E_n(\mathbf{0})\delta_{nn'} + \frac{\hbar^2}{2m_0^2}\sum_{n''}\left[\frac{\mathbf{k}\cdot\mathbf{p}_{nn''}\,\mathbf{k}\cdot\mathbf{p}_{n''n'}}{[E_{n'}(\mathbf{0}) - E_{n''}(\mathbf{0})]} + \frac{\mathbf{k}\cdot\mathbf{p}_{nn''}\,\mathbf{k}\cdot\mathbf{p}_{n''n'}}{[E_n(\mathbf{0}) - E_{n''}(\mathbf{0})]}\right]\\ &= \left[E_n(\mathbf{0}) + \frac{\hbar^2}{2}\sum_{\alpha\beta}k_\alpha\left(\frac{1}{m_n}\right)_{\alpha\beta}k_\beta\right]\delta_{nn'} + \text{interband terms of order } k^2,\end{aligned}$$

which is, of course, the same as Eq. (2.11).

We now restrict ourselves to zincblende and diamond crystals for which $n = s = \Gamma_1$ (see Appendix B for the symmetry properties), $p_{nn} = 0$, and

$$E(\mathbf{k}) = E_{\Gamma_1} + \frac{\hbar^2 k^2}{2m_0} + \frac{\hbar^2}{m_0^2}\sum_l{}' \frac{|\mathbf{p}_{\Gamma_1 l}\cdot\mathbf{k}|^2}{E_{\Gamma_1} - E_l}. \tag{2.24}$$

Note that, for conciseness, we are also only using the group notation for the electron states in a zincblende crystal. The standard state ordering for zincblende and diamond is given in Fig. 2.1. There are exceptions to these such as the inverted band structure of HgTe [9] and the inverted conduction band of Si. Thus, the interaction of the Γ_1 state with other states via $p_{\Gamma_1 l}$ changes the dispersion relation from that of a free-electron one. The new inverse effective-mass tensor is

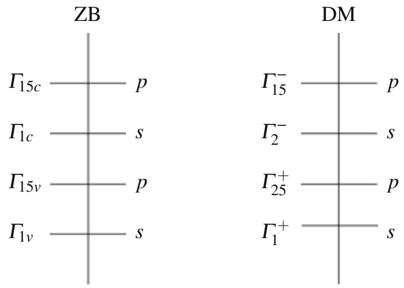

Fig. 2.1 Zone-center states for typical zincblende (ZB) and diamond (DM) crystals

$$\left(\frac{1}{m^*}\right)_{ij} = \frac{1}{m_0}\delta_{ij} + \frac{2}{m_0^2}\sum_l{}' \frac{p^i_{\Gamma_1 l} p^j_{l\Gamma_1}}{E_{\Gamma_1} - E_l}. \tag{2.25}$$

Equation (2.11) or Eqs. (2.24) and (2.25) define the one-band, effective-mass model. The band dispersion can be calculated given the momentum matrix elements and band gaps. Note that Eq. (2.24) is only approximate, giving the parabolic approximation. Constraints on the effective mass can now be written from Eq. (2.25).

2.5 Effective Masses

One can write down simple expressions for the effective masses of nondegenerate bands.

2.5.1 Electron

Because of the energy denominator, distant bands are expected to be less important. The two closest bands to the Γ_{1c} state for cubic semiconductors are the Γ_{15} states $\sim X, Y, Z$. Since $\Gamma_{1c} \sim S$, and

$$\langle S|p_x|X\rangle = \langle S|p_y|Y\rangle = \langle S|p_z|Z\rangle,$$

the conduction mass m_e is isotropic:

$$\begin{aligned}\frac{1}{m_e} &= \frac{1}{m_0} + \frac{2}{m_0^2}\frac{|\langle S|p_x|X_v\rangle|^2}{E_{\Gamma_{1c}} - E_{\Gamma_{15v}}} + \frac{2}{m_0^2}\frac{|\langle S|p_x|X_c\rangle|^2}{E_{\Gamma_{1c}} - E_{\Gamma_{15c}}} \\ &\equiv \frac{1}{m_0} + \frac{2P^2}{\hbar^2 E_0} - \frac{2P'^2}{\hbar^2 E_0'},\end{aligned} \tag{2.26}$$

where

$$P^2 = \frac{\hbar^2}{m_0^2}|\langle S|p_x|X_v\rangle|^2, \tag{2.27}$$

$$P'^2 = \frac{\hbar^2}{m_0^2}|\langle S|p_x|X_c\rangle|^2. \tag{2.28}$$

For diamond,

$$P' = 0 \quad \Longrightarrow \quad 0 < m_e < m_0.$$

For zincblende, typically

$$\frac{P'^2}{E'_0} < \frac{P^2}{E_0} \quad \Longrightarrow \quad 0 < m_e < m_0.$$

Hence, the electron effective mass is usually smaller than the free-electron mass.

2.5.2 Light Hole

Of the three-fold degenerate Γ_{15v} states, only one couples with Γ_{1c} along a given Δ direction, giving rise to the light-hole (lh) mass. Consider $\mathbf{k} = (k_x, 0, 0)$. Then, since the lh state can now be assumed nondegenerate, again m_{lh} is isotropic (though a more accurate model will reveal them to be anisotropic):

$$\frac{1}{m_{lh}} = \frac{1}{m_0} + \frac{2}{m_0^2}\frac{|\langle S|p_x|X_v\rangle|^2}{E_{\Gamma_{15v}} - E_{\Gamma_{1c}}} = \frac{1}{m_0} - \frac{2P^2}{\hbar^2 E_0} \equiv \frac{1}{m_0}\left(1 - \frac{E_P}{E_0}\right), \tag{2.29}$$

with

$$E_P \equiv \frac{2m_0 P^2}{\hbar^2} \tag{2.30}$$

known as the Kane parameter. Typically, $E_p \sim 20\,\text{eV}$, $E_0 \sim 0$–$5\,\text{eV}$. Hence, $-m_0 < m_{lh} < 0$. Note that, contrary to the electron case, the lh mass does not contain the P' term.

To compare the lh and e masses,

$$\frac{1}{m_e} + \frac{1}{m_{lh}} = \frac{2}{m_0} - \frac{2P'^2}{\hbar^2 E'_0} = \frac{1}{m_0}\left(2 - \frac{E'_P}{E'_0}\right).$$

For diamond, $E'_P = 0$, giving

$$\frac{1}{m_e} + \frac{1}{m_{lh}} > 0 \quad \text{(always)}, \tag{2.31}$$

and

$$|m_{lh}| > m_e. \tag{2.32}$$

For zincblende, $E'_P \sim 1$–$10\,\text{eV}$, $E'_0 \sim 3$–$5\,\text{eV}$, and the masses are closer in magnitude. The qualitative effect of the e–lh interaction on the effective masses is sketched in Fig. 2.2. This is also known as a two-band model.

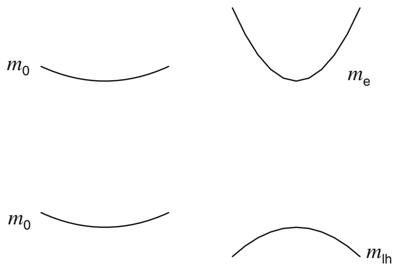

Fig. 2.2 Two-band model. The $k \cdot p$ interaction changes the curvatures

2.5.3 Heavy Hole

One may define the heavy-hole (hh) states as the partners in the Γ_{15v} representation which do not couple to the conduction s electron. In so far as the Γ_{15c} states are not considered, the hh state has the free-electron mass. Including the Γ_{15c} state and again assuming that the Γ_{15v} states are nondegenerate, the isotropic mass is

$$\frac{1}{m_{hh}} = \frac{1}{m_0} - \frac{2}{m_0^2}\frac{|\langle Y_v|p_x|Z_c\rangle|^2}{E_0 + E_0'} = \frac{1}{m_0}\left(1 - \frac{E_Q}{E_0 + E_0'}\right). \tag{2.33}$$

Typically, $E_Q \sim$20–25 eV, $E_0 + E_0' \sim 10\,\text{eV}$, and $0 > m_{hh} > -m_0$.

We have seen how the simple one-band model can provide a semi-quantitative description of various bands for zincblende and diamond semiconductors, particularly the sign and relative magnitudes of the associated effective masses. The necessity of describing the band structure quantitatively and more accurately (such as nonparabolicity and anisotropy) leads to the consideration of multiband models.

2.6 Nonparabolicity

So far, we have presented the simplest one-band model in order to illustrate the theory; it does allow for anisotropy via an anisotropic effective mass. Still, a one-band model can be made to reproduce more detailed features of a real band including nonparabolicity, anisotropy and spin splitting. An example of such a model is the k^4 dispersion relation given by Rössler [23]:

$$\begin{aligned} E(\mathbf{k}) = \tfrac{\hbar^2 k^2}{2m^*} &+ \alpha k^4 + \beta\left(k_y^2k_z^2 + k_z^2k_x^2 + k_x^2k_y^2\right) \\ &\pm\ \gamma\left\{k^2\left(k_y^2k_z^2 + k_z^2k_x^2 + k_x^2k_y^2\right) - 9k_x^2k_y^2k_z^2\right\}^{1/2}. \end{aligned} \tag{2.34}$$

The first term on the right-hand side is the familiar isotropic and parabolic effective-mass term. The remaining terms give nonparabolicity, warping and spin splitting, respectively. We will derive them later in the book.

2.7 Summary

We have set up the fundamental $k \cdot p$ equation and shown, using a variety of techniques, how a one-band model (the so-called effective-mass model) can be obtained from it. This model was then used to derive a semi-quantitative understanding of the magnitude of the effective masses of band-edge states for cubic semiconductors. In particular, it was shown that the simplest effective-mass model for electrons and light holes gives isotropic masses.

Chapter 3
Perturbation Theory – Valence Band

3.1 Overview

Degenerate perturbation theory is presented in order to derive the valence-band Hamiltonian. This will be illustrated in detail for the Dresselhaus–Kip–Kittel Hamiltonian for diamond and for the valence-band Hamiltonian for wurtzite.

3.2 Dresselhaus–Kip–Kittel Model

We first give the derivation of the 3×3 (i.e., no spin) Dresselhaus–Kip–Kittel (DKK) Hamiltonian using the original second-order degenerate perturbation theory approach [2]. The theory applies to the valence band of diamond.

3.2.1 Hamiltonian

The starting equation is the $k \cdot p$ equation, Eq. (2.6), without the spin-orbit term:

$$\left[\frac{p^2}{2m_0} + V(\mathbf{r}) + \frac{\hbar}{m_0}\mathbf{k} \cdot \mathbf{p}\right] u_{n\mathbf{k}}(\mathbf{r}) = \mathcal{E}_n(\mathbf{k}) u_{n\mathbf{k}}(\mathbf{r}).$$

The unperturbed $u^r_{n\mathbf{0}}(\mathbf{r}) \equiv \varepsilon^+_r$ are the three-fold degenerate solutions at the zone center or Γ point. They transform according to the Γ^+_{25} irreducible representation (Fig. 3.1). The three states are: $\varepsilon^+_1 \sim yz$, $\varepsilon^+_2 \sim zx$, $\varepsilon^+_3 \sim xy$; they are even with respect to the inversion operator. An atomistic description of the transformation properties of some of the states of the DM structure is given in Table 3.1. Since the unperturbed states are degenerate, we have to use degenerate perturbation theory to find the solutions at finite $\mathbf{k}$.

The first-order correction is given by the matrix elements

$$\sim \langle \varepsilon^+_r | \mathbf{k} \cdot \mathbf{p} | \varepsilon^+_s \rangle = 0$$

L.C. Lew Yan Voon, M. Willatzen, *The* k · p *Method*,
DOI 10.1007/978-3-540-92872-0_3, © Springer-Verlag Berlin Heidelberg 2009

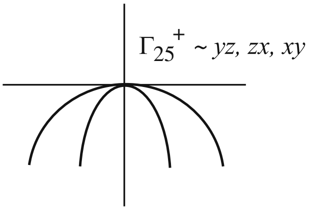

Fig. 3.1 Three-band model for diamond-type semiconductors

Table 3.1 Symmetries of states at the Γ point for diamond structure [5, 24]. The second column gives the orbitals on the two atoms in the basis. The far-right column gives the corresponding plane-wave states

		Cardona and Pollak [5]		
Γ_1^+	$s_a + s_a'$	Γ_1^l	s^+	[000]
Γ_{25}^+	$p_a - p_a' \sim yz, zx, xy$	$\Gamma_{25'}^l$	p^+	[111]
Γ_2^-	$s_a - s_a' \sim xyz$	$\Gamma_{2'}^l$	s^-	[111]
Γ_{15}^-	$p_a + p_a' \sim x, y, z$	Γ_{15}	p^-	[111]
Γ_{12}^-	$d_a - d_a' \sim \sqrt{3}\left(y^2 - z^2\right), 3x^2 - r^2$	$\Gamma_{12'}$	d^-	[200]
Γ_1^+	$s_a + s_a'$	Γ_1^u	s^+	[111]
Γ_{25}^+	$d_a + d_a' \sim yz, zx, xy$	$\Gamma_{25'}^u$	d^+	[200]
Γ_2^-	$s_a - s_a' \sim xyz$	$\Gamma_{2'}^u$	s^-	[200]

since the ε_r^+'s have the same parity and $\mathbf{p}$ is odd under inversion. In the language of group theory, one says that $\Gamma_{25}^+ \otimes \Gamma_{15}^- \otimes \Gamma_{25}^+$ does not contain Γ_1^+.

One, therefore, needs second-order degenerate perturbation theory. The corrections to the cellular functions and matrix elements are:

$$u_{n\mathbf{k}}^r = \varepsilon_r^+ + \frac{\hbar}{m_0}\mathbf{k} \cdot \sideset{}{'}\sum_{l\alpha\nu} \frac{|l\alpha\nu\rangle\langle l\alpha\nu|\mathbf{p}|r\rangle}{E_{\Gamma_{25}^+} - E_{l\alpha}}, \tag{3.1}$$

$$\begin{aligned} H_{rs} \equiv \langle r|H(\mathbf{k})|s\rangle &= \frac{\hbar^2}{m_0^2} \sideset{}{'}\sum_{l\alpha\nu} \frac{\langle r|\mathbf{k}\cdot\mathbf{p}|l\alpha\nu\rangle\langle l\alpha\nu|\mathbf{k}\cdot\mathbf{p}|s\rangle}{E_{\Gamma_{25}^+} - E_{l\alpha}} \\ &= \frac{\hbar^2}{m_0^2} k_i k_j \sideset{}{'}\sum_{l\alpha\nu} \frac{\langle r|p_i|l\alpha\nu\rangle\langle l\alpha\nu|p_j|s\rangle}{E_{\Gamma_{25}^+} - E_{l\alpha}}, \end{aligned} \tag{3.2}$$

where $|r\rangle = u_{n\mathbf{0}}^r$, $l\alpha\nu$ denotes the state ν (in case of degeneracy) belonging to the α representation in the band l; $E_{l\alpha}$ is the energy of that state at $\mathbf{k} = \mathbf{0}$. $E_{\Gamma_{25}^+}$ is the energy of the ε_r^+ states. The diagonal perturbation matrix elements are given by

$$H_{rr} = \frac{\hbar^2}{m_0^2} k_i k_j \sideset{}{'}\sum_{l\alpha\nu} \frac{\langle r|p_i|l\alpha\nu\rangle\langle l\alpha\nu|p_j|r\rangle}{E_{\Gamma_{25}^+} - E_{l\alpha}}.$$

In the group of DM, there are operators that invert all three coordinates or just one; taking, e.g., $r = xy$ (the others follow by permutation),

$$\langle xy|p_i|l\alpha\nu\rangle\langle l\alpha\nu|p_j|xy\rangle$$

is nonzero only if all coordinates appear pairwise. For example, in

$$\langle xy|p_x|l\alpha\nu\rangle\langle l\alpha\nu|p_j|xy\rangle,$$

using an operator that only changes the sign of x requires $p_j = p_x$ (equivalently for p_y), while in

$$\langle xy|p_z|l\alpha\nu\rangle\langle l\alpha\nu|p_j|xy\rangle,$$

using an operator that only changes the sign of z requires $p_j = p_z$. Thus, $p_i = p_j$ and two independent choices are $p_i = p_y (= p_x)$, p_z. Therefore,

$$H_{33} = \frac{\hbar^2}{m_0^2} \sum_{l\alpha\nu}{}' \left\{ k_z^2 \frac{|\langle xy|p_z|l\alpha\nu\rangle|^2}{E_{\Gamma_{25}^+} - E_{l\alpha}} + \left(k_x^2 + k_y^2\right) \frac{|\langle xy|p_y|l\alpha\nu\rangle|^2}{E_{\Gamma_{25}^+} - E_{l\alpha}} \right\}.$$

For the off-diagonal matrix elements, one again requires the coordinates to appear pairwise. For example, for $r = xy$ and $s = yz$,

$$\langle xy|p_x|l\alpha\nu\rangle\langle l\alpha\nu|p_j|yz\rangle,$$

using an operator that only changes the sign of x requires $p_j = p_y$ or p_z but, in addition, using an operator that only changes the sign of y requires $p_j = p_z$ only. One, therefore, gets

$$H_{31} = \frac{\hbar^2}{m_0^2} k_x k_z \sum_{l\alpha\nu}{}' \left\{ \frac{\langle xy|p_z|l\alpha\nu\rangle\langle l\alpha\nu|p_x|yz\rangle + \langle xy|p_x|l\alpha\nu\rangle\langle l\alpha\nu|p_z|yz\rangle}{E_{\Gamma_{25}^+} - E_{l\alpha}} \right\}.$$

Thus, one can introduce three independent parameters:

$$\begin{aligned} L &\equiv \frac{\hbar^2}{m_0^2} \sum_{l\alpha\nu}{}' \frac{|\langle xy|p_z|l\alpha\nu\rangle|^2}{E_{\Gamma_{25}^+} - E_{l\alpha}}, \\ M &\equiv \frac{\hbar^2}{m_0^2} \sum_{l\alpha\nu}{}' \frac{|\langle xy|p_y|l\alpha\nu\rangle|^2}{E_{\Gamma_{25}^+} - E_{l\alpha}}, \\ N &\equiv \frac{\hbar^2}{m_0^2} \sum_{l\alpha\nu}{}' \frac{\langle xy|p_z|l\alpha\nu\rangle\langle l\alpha\nu|p_x|yz\rangle + \langle xy|p_x|l\alpha\nu\rangle\langle l\alpha\nu|p_z|yz\rangle}{E_{\Gamma_{25}^+} - E_{l\alpha}}, \end{aligned} \tag{3.3}$$

giving rise to the DKK Hamiltonian:

$$H_{\mathrm{DKK}}(\mathbf{k}) = \left(\begin{array}{ccc} |yz\rangle & |zx\rangle & |xy\rangle \\ Lk_x^2 + M(k_y^2 + k_z^2) & Nk_xk_y & Nk_xk_z \\ Nk_xk_y & Lk_y^2 + M(k_z^2 + k_x^2) & Nk_yk_z \\ Nk_xk_z & Nk_yk_z & Lk_z^2 + M(k_x^2 + k_y^2) \end{array} \right). \tag{3.4}$$

The band energies are then given by

$$E_n(\mathbf{k}) = E_{\Gamma_{25}^+} + \frac{\hbar^2 k^2}{2m_0} + \lambda,$$

where λ are the eigenvalues of the DKK Hamiltonian. Luttinger and Kohn (LK) [6] came up with a slightly different notation for the Hamiltonian, which includes the free-electron term. They give the matrix as D with matrix elements

$$D_{mn} = D_{mn}^{ij} k_i k_j, \tag{3.5}$$

$$D_{mn}^{ij} = \frac{\hbar^2}{2m_0} \left[\delta_{mn}\delta_{jj'} + \frac{1}{m_0} \sum_l^B \frac{p_{ml}^i p_{ln}^j + p_{ml}^j p_{ln}^i}{E_{\Gamma_{25}^+} - E_l} \right]. \tag{3.6}$$

Then

$$D = \left(\begin{array}{ccc} |yz\rangle & |zx\rangle & |xy\rangle \\ A_L k_x^2 + B_L \left(k_y^2 + k_z^2\right) & C_L k_x k_y & C_L k_x k_z \\ C_L k_x k_y & A_L k_y^2 + B_L \left(k_z^2 + k_x^2\right) & C_L k_y k_z \\ C_L k_x k_z & C_L k_y k_z & A_L k_z^2 + B_L \left(k_x^2 + k_y^2\right) \end{array} \right), \tag{3.7}$$

with

$$\begin{aligned} A_L &= \frac{\hbar^2}{2m_0} + \frac{\hbar^2}{m_0^2} \sum_l \frac{p_{1l}^x p_{l1}^x}{E_{\Gamma_{25}^+} - E_l}, \\ B_L &= \frac{\hbar^2}{2m_0} + \frac{\hbar^2}{m_0^2} \sum_l \frac{p_{1l}^y p_{l1}^y}{E_{\Gamma_{25}^+} - E_l}, \\ C_L &= \frac{\hbar^2}{2m_0^2} \sum_l \frac{p_{1l}^x p_{l2}^y + p_{1l}^y p_{l2}^x}{E_{\Gamma_{25}^+} - E_l}. \end{aligned} \tag{3.8}$$

Thus, the LK parameters are related to the DKK ones via

$$A_L = L + \frac{\hbar^2}{2m_0},$$

$$\begin{aligned} B_L &= M + \frac{\hbar^2}{2m_0}, \\ C_L &= N. \end{aligned} \tag{3.9}$$

Terms of higher order, for example, k^4, have been considered by some authors [25] but will not be discussed in this book as they are not commonly used in the literature.

3.2.2 Eigenvalues

The DKK Hamiltonian cannot be diagonalized analytically throughout the first Brillouin zone (FBZ). However, analytical solutions exist when there is double degeneracy (e.g., along $L - \Gamma - X$). We now obtain those solutions:

$$\begin{vmatrix} Lk_x^2 + M\left(k_y^2 + k_z^2\right) - \lambda & Nk_xk_y & Nk_xk_z \\ Nk_xk_y & Lk_y^2 + M\left(k_z^2 + k_x^2\right) - \lambda & Nk_yk_z \\ Nk_xk_z & Nk_yk_z & Lk_z^2 + M\left(k_x^2 + k_y^2\right) - \lambda \end{vmatrix}$$

$$\begin{aligned} &= \left[Lk_x^2 + M\left(k_y^2 + k_z^2\right) - \lambda\right]\left[Lk_y^2 + M(k_x^2 + k_z^2) - \lambda\right]\left[Lk_z^2 + M\left(k_y^2 + k_x^2\right) - \lambda\right] \\ &\quad - \left[Lk_x^2 + M\left(k_y^2 + k_z^2\right) - \lambda\right]N^2k_y^2k_z^2 - \left[Lk_z^2 + M\left(k_x^2 + k_y^2\right) - \lambda\right]N^2k_x^2k_y^2 \\ &\quad - \left[Lk_y^2 + M\left(k_x^2 + k_z^2\right) - \lambda\right]N^2k_x^2k_z^2 + 2N^3k_x^2k_y^2k_z^2 = 0. \end{aligned}$$

Using

$$[a - \lambda][b - \lambda][c - \lambda] = abc - (ac + bc + ab)\lambda + (a + b + c)\lambda^2 - \lambda^3,$$

we have

$$\begin{aligned} &\lambda^3 - (L + 2M)k^2\lambda^2 \\ &\quad + \Big\{\left[Lk_x^2 + M\left(k_y^2 + k_z^2\right)\right]\left[Lk_y^2 + M\left(k_x^2 + k_z^2\right)\right] \\ &\quad + \left[Lk_x^2 + M\left(k_y^2 + k_z^2\right)\right]\left[Lk_z^2 + M\left(k_x^2 + k_y^2\right)\right] \\ &\quad + \left[Lk_y^2 + M\left(k_x^2 + k_z^2\right)\right]\left[Lk_z^2 + M\left(k_x^2 + k_y^2\right)\right] - N^2\left(k_x^2k_y^2 + k_x^2k_z^2 + k_y^2k_z^2\right)\Big\}\lambda \\ &\quad - \Big\{\left[Lk_x^2 + M\left(k_y^2 + k_z^2\right)\right]\left[Lk_y^2 + M\left(k_x^2 + k_z^2\right)\right]\left[Lk_z^2 + M\left(k_x^2 + k_y^2\right)\right] \\ &\quad + N^2\left[Lk_x^2 + M\left(k_y^2 + k_z^2\right)\right]k_y^2k_z^2 + N^2\left[Lk_y^2 + M\left(k_x^2 + k_z^2\right)\right]k_x^2k_z^2 \\ &\quad + N^2\left[Lk_z^2 + M\left(k_y^2 + k_x^2\right)\right]k_x^2k_y^2 - 2N^3k_x^2k_y^2k_z^2\Big\} = 0. \end{aligned} \tag{3.10}$$

This general characteristic equation is too complicated to be of much use. However, when there is a degenerate pair of eigenvalues,

$$(\lambda - a)^2(\lambda - b) = \lambda^3 - (2a + b)\lambda^2 + (2ab + a^2)\lambda - a^2 b = 0.$$

Comparing with Eq. (3.10), one has

$$\begin{aligned} 2a + b &= (L + 2M)k^2, && (3.11)\\ 2ab + a^2 &= \left(L^2 - N^2 + 3M^2 + 2ML\right) k_{xyz} + \left(M^2 + 2LM\right)\left(k_x^4 + k_y^4 + k_z^4\right) \\ &\equiv \alpha && (3.12) \end{aligned}$$

where $k_{xyz} = k_x^2 k_y^2 + k_y^2 k_z^2 + k_z^2 k_x^2$. Eliminating b from Eqs. (3.11) and (3.12) gives

$$3a^2 - 2(L + 2M)k^2 a + \alpha = 0,$$

and

$$\begin{aligned} a &= \frac{(L + 2M)}{3}k^2 \pm \left[\frac{(L + 2M)^2}{9}k^4 - \frac{\alpha}{3}\right]^{1/2} \\ &= \frac{(L + 2M)}{3}k^2 \pm \left[\frac{(L - M)^2}{9}k^4 + \frac{1}{3}\left[N^2 - (L - M)^2\right]\left(k_x^2 k_y^2 + k_y^2 k_z^2 + k_z^2 k_x^2\right)\right]^{1/2}. \end{aligned}$$

Hence,

$$E(\mathbf{k}) = Ak^2 \pm \left[B^2 k^4 + C^2\left(k_y^2 k_z^2 + k_z^2 k_x^2 + k_x^2 k_y^2\right)\right]^{1/2}, \qquad (3.13)$$

where

$$A \equiv \frac{(L + 2M)}{3} + \frac{\hbar^2}{2m_0}, B^2 \equiv \frac{(L - M)^2}{9}, C^2 \equiv \frac{1}{3}\left[N^2 - (L - M)^2\right]. \qquad (3.14)$$

This (restricted) result will turn out to be identical to the spin case. Note that the dispersion is both anisotropic (if $C \neq 0$) and nonparabolic (if $B, C \neq 0$); the first property is also known as warping. A careful study of warping was given in [26].

3.2.3 L, M, N Parameters

We next study the L, M, N parameters more closely. The matrix elements involved are

$$\langle r|\mathbf{p}|l\rangle \sim \Gamma_{25}^{+} \otimes \Gamma_{15}^{-} \otimes \Gamma^{l}.$$

From Table 3.2, one deduces that

$$\Gamma_{25}^{+} \otimes \Gamma_{15}^{-} \sim \Gamma_{12}^{-} \oplus \Gamma_{15}^{-} \oplus \Gamma_{2}^{-} \oplus \Gamma_{25}^{-}; \qquad (3.15)$$

in effect, all the odd-parity representations except for Γ_1^-. In order, to be able to get Γ_1^+ in the decomposition, Γ^l must clearly have odd parity; however, Γ_1^- is not appropriate since the decomposition will then not include Γ_1^+. Otherwise, all of the four irreducible representations on the right-hand side of Eq. (3.15) can interact with the valence-band edge.

Table 3.2 Character table of the group O_h

O_h	E	$8C_3$	$3C_2$	$6C_4$	$6C_2'$	I	$8S_6 =$ IC_3	$3\sigma_h =$ IC_4^2	$6S_4 =$ IC_4	$6\sigma_d =$ IC_2
Γ_1^+	1	1	1	1	1	1	1	1	1	1
Γ_2^+	1	1	1	–1	–1	1	1	1	–1	–1
Γ_{12}^+	2	–1	2	0	0	2	–1	2	0	0
Γ_{15}^+	3	0	–1	1	–1	3	0	–1	1	–1
Γ_{25}^+	3	0	–1	–1	1	3	0	–1	–1	1
Γ_1^-	1	1	1	1	1	–1	–1	–1	–1	–1
Γ_2^-	1	1	1	–1	–1	–1	–1	–1	1	1
Γ_{12}^-	2	–1	2	0	0	–2	1	–2	0	0
Γ_{15}^-	3	0	–1	1	–1	–3	0	1	–1	1
Γ_{25}^-	3	0	–1	–1	1	–3	0	1	1	–1

The band-edge structure for diamond-type semiconductors is believed to be as given in Fig. 3.2. The state Γ_{12}^- was reported by von der Lage and Bethe [27] to have as smallest $l = 5$. However, Herman [28] showed that it originates from $\langle 200 \rangle$ plane waves and as having the symmetry of d^- states. The discrepancy is likely due to the fact that von der Lage and Bethe were really studying the cubic group with a single atom (ion) per unit cell whereas Herman considered the case of two atoms per unit cell. Thus, one expects the maximum perturbation from the Γ_2^-, Γ_{12}^-, Γ_{15}^- bands; in particular, there is no perturbation from, e.g., Γ_1^+.

Similarly, not all states appear in the summation for the DKK parameters. Hence, instead of writing the DKK Hamiltonian in terms of the L, M, N, one can also write it in terms of interband parameters between states of given symmetries; furthermore, this will provide relations among the L, M, N parameters.

3.2.3.1 *L* Parameter

Starting with L, only Γ_2^- and Γ_{12}^- can contribute. This can be ascertained by looking at the reflection properties of the matrix element. Consider, e.g., $|r\rangle = |yz\rangle$. Then

$$p_x |yz\rangle \sim xyz \sim \Gamma_2^- .$$

Under an IC_4^2 reflection, Γ_{15}^- and Γ_{25}^- are even, while Γ_2^- is odd (see Table 3.2). This eliminates the former two representations from the matrix elements for L. This can be shown more explicitly, e.g., for the Γ_{15}^- representation ($\sim x, y, z$):

$$\langle yz | p_x | x, z \rangle = 0$$

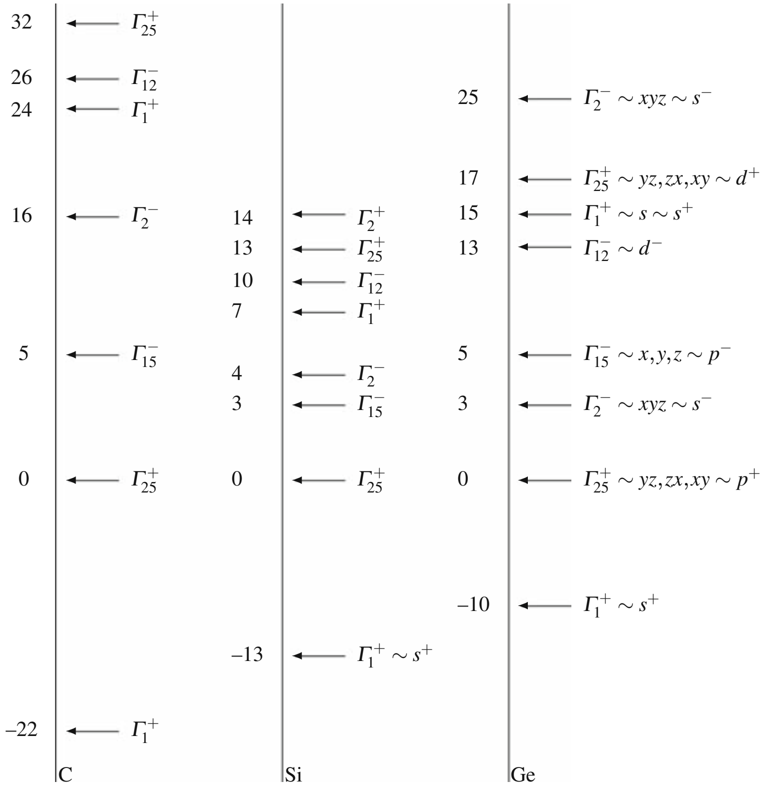

Fig. 3.2 Schematic of zone-center energy (in eV) ordering for diamond-structure semiconductors (not to scale; C from Willatzen et al. [29], Si from Cardona and Pollak [5], Ge from DKK [2])

using IC_{2y} and

$$\langle yz|p_x|y\rangle = 0$$

using IC_{2x}. We now wish to consider how many independent interband terms there are. Consider first

$$L = \frac{\hbar^2}{m_0^2} {\sum_l}' \left\{ \frac{|\langle yz|p_x|\beta_l^-\rangle|^2}{E_{\Gamma_{25}^+} - E_l} + \sum_\nu \frac{|\langle yz|p_x|\gamma_{\nu l}^-\rangle|^2}{E_{\Gamma_{25}^+} - E_l} \right\}, \tag{3.16}$$

where $\beta_l^- \in \Gamma_2^-$ and $\gamma_{\nu l}^- \in \Gamma_{12}^-$. DKK showed that each representation only contributes one matrix element per band, independent of its dimension. We will now obtain this result. Let

$$F \equiv \frac{\hbar^2}{m_0^2} {\sum_{l\in\Gamma_2^-}}' \frac{|\langle yz|p_x|\beta_l^-\rangle|^2}{E_{\Gamma_{25}^+} - E_l}, \tag{3.17}$$

$$G \equiv \frac{\hbar^2}{m_0^2} \sum_{l \in \Gamma_{12}^-}{}' \frac{|\langle yz|p_x|\gamma_{1l}^-\rangle|^2}{E_{\Gamma_{25}^+} - E_l}. \tag{3.18}$$

Since Γ_2^- is one dimensional, there is only one such term. On the other hand, Γ_{12}^- is two dimensional; it turns out this still only contributes one distinct term. To establish this result, we need the basis functions. One could choose the d-like functions (as done by von der Lage and Bethe); however, the latter do not generate a unitary irreducible representation [2]. Hence, we follow DKK in choosing $\gamma_{\nu l}^-$ such that

$$\gamma_1^- = x^2 + \omega y^2 + \omega^2 z^2, \tag{3.19}$$

$$\gamma_2^- = x^2 + \omega^2 y^2 + \omega z^2, \tag{3.20}$$

where $\omega^3 = 1$ and $\gamma_\nu^- = \gamma_\nu - \gamma_\nu'$. To verify that they are basis functions for the Γ_{12}^- irreducible representation, one can generate the representation matrices and show that they have the right character vector. We use

$$\mathcal{O}(R) f_i(\mathbf{r}) = f(\mathsf{R}^{-1}\mathbf{r}) = \sum_j f_j(\mathbf{r}) \mathsf{R}_{ji},$$

where R is a rotation. For example (note that we only need the matrix for one element in each class):

$$\begin{aligned}
\mathcal{O}(C_{4x})\gamma_1^- &= C_{4x}^{-1}\gamma_1^- = C_{4x}^{-1}\left(x^2 + \omega y^2 + \omega^2 z^2\right)^- \overset{x\bar{z}y}{=} \left(x^2 + \omega z^2 + \omega^2 y^2\right)^- = \gamma_2^-, \\
\mathcal{O}(C_{4x})\gamma_2^- &= \gamma_1^-, \\
\Longrightarrow \quad C_{4x} &= \begin{pmatrix} 0 & 1 \\ 1 & 0 \end{pmatrix}, \\
\mathcal{O}(C_{4y}^{-1})\gamma_1^- &= C_{4y}\left(x^2 + \omega y^2 + \omega^2 z^2\right)^- \overset{\bar{z}yx}{=} \left(z^2 + \omega y^2 + \omega^2 x^2\right)^- \\
&= \frac{1}{\omega}\left(x^2 + \omega^2 y^2 + \omega z^2\right)^- = \frac{1}{\omega}\gamma_2^-, \\
\mathcal{O}\left(C_{4y}^{-1}\right)\gamma_2^- &= C_{4y}\left(x^2 + \omega z^2 + \omega^2 y^2\right)^- = \left(z^2 + \omega x^2 + \omega^2 y^2\right)^- \\
&= \frac{1}{\omega^2}\left(x^2 + \omega y^2 + \omega^2 z^2\right)^- = \frac{1}{\omega^2}\gamma_1^-, \\
\Longrightarrow \quad C_{4y}^{-1} &= \begin{pmatrix} 0 & \frac{1}{\omega} \\ \frac{1}{\omega^2} & 0 \end{pmatrix}, \\
\mathcal{O}(C_2)\gamma_i^- &= \gamma_i^-, \\
\Longrightarrow \quad C_2 &= \begin{pmatrix} 1 & 0 \\ 0 & 1 \end{pmatrix},
\end{aligned}$$

$$\begin{aligned}\mathcal{O}\left(C_{3xyz}\right)\gamma_1^- &= C_{3xyz}^{-1}\left(x^2+\omega y^2+\omega^2 z^2\right)^- \overset{zxy}{=} \left(z^2+\omega x^2+\omega^2 y^2\right)^- \\ &= \frac{1}{\omega^2}\left(x^2+\omega y^2+\omega^2 z^2\right)^- = \frac{1}{\omega^2}\gamma_1^-, \\ \mathcal{O}\left(C_{3xyz}\right)\gamma_2^- &= \left(z^2+\omega y^2+\omega^2 x^2\right)^- = \frac{1}{\omega}\gamma_2^-, \\ \Longrightarrow \quad C_{3xyz} &= \begin{pmatrix} \frac{1}{\omega^2} & 0 \\ 0 & \frac{1}{\omega} \end{pmatrix} = \begin{pmatrix} \omega & 0 \\ 0 & \omega^2 \end{pmatrix}.\end{aligned}$$

C_2' is similar to C_4, and so on. In order to get the characters, we have, for example for C_{3xyz}

$$\chi(C_{3xyz}) = \omega + \omega^2 = -1,$$

since $\omega + \omega^2 + \omega^3 = 0$ and $\omega^3 = 1$. Also, one should check that the representation is indeed unitary (i.e., $U^\dagger = U^{-1}$). For example, given C_{4y}^{-1} above and assuming unitarity,

$$C_{4y}^\dagger = C_{4y}^{-1} = \begin{pmatrix} 0 & \frac{1}{\omega^{*2}} \\ \frac{1}{\omega^*} & 0 \end{pmatrix} = \begin{pmatrix} 0 & \frac{1}{\omega} \\ \frac{1}{\omega^2} & 0 \end{pmatrix},$$

since

$$\omega^3 = 1 \Longrightarrow \quad \frac{1}{\omega^{*2}} = \omega^*,$$

and

$$\omega = \mathrm{e}^{\mathrm{i}\theta} \Longrightarrow \quad \omega^* = 1/\omega.$$

Also

$$C_{4y} = (C_{4y}^\dagger)^\dagger = \begin{pmatrix} 0 & \frac{1}{\omega} \\ \frac{1}{\omega^2} & 0 \end{pmatrix},$$

and

$$C_{4y}C_{4y}^{-1} = C_{4y}C_{4y}^\dagger = \begin{pmatrix} 0 & \frac{1}{\omega} \\ \frac{1}{\omega^2} & 0 \end{pmatrix}\begin{pmatrix} 0 & \frac{1}{\omega} \\ \frac{1}{\omega^2} & 0 \end{pmatrix} = \begin{pmatrix} \frac{1}{\omega^3} & 0 \\ 0 & \frac{1}{\omega^3} \end{pmatrix} = \begin{pmatrix} 1 & 0 \\ 0 & 1 \end{pmatrix}.$$

Thus $\gamma_{vl}^- \sim \Gamma_{12}^-$.

Now, following DKK, let

$$\langle yz|p_x|\gamma_1^-\rangle \equiv R. \tag{3.21}$$

We will show that $\langle yz|p_x|\gamma_2^-\rangle$ is related. To wit,

$$\begin{aligned}C_{4x}\langle yz|p_x|\gamma_2^-\rangle &= C_{4x}\langle yz|p_x|(x^2+\omega^2y^2+\omega z^2)^-\rangle = -\langle yz|p_x|(x^2+\omega y^2+\omega^2z^2)^-\rangle\\ &= -R.\end{aligned}$$

The two matrix elements with respect to the two degenerate states are, therefore, the same up to a sign giving

$$L = F + 2G. \tag{3.22}$$

3.2.3.2 *M* Parameter

Similarly, one can show that M only has contributions from Γ_{15}^- and Γ_{25}^- (lowest $l = 3$ [27]). Again, taking the Γ_{15}^- representation as example:

$$\langle yz|p_y|x\rangle = 0$$

using IC_{2x},

$$\langle yz|p_y|y\rangle = 0$$

using IC_{2y}, but

$$\langle yz|p_y|z\rangle \neq 0 \;\forall\; IC_2.$$

Then,

$$M = \frac{\hbar^2}{m_0^2}\sum_{lv}{}^{'}\left\{\frac{|\langle yz|p_y|lv\rangle|^2}{E_{\Gamma_{25}^+}-E_{\Gamma_{15}^-}} + \frac{|\langle yz|p_y|lv\rangle|^2}{E_{\Gamma_{25}^+}-E_{\Gamma_{25}^-}}\right\}. \tag{3.23}$$

Let

$$H_1 \equiv \frac{\hbar^2}{m_0^2}\sum_{l}{}^{'}\frac{|\langle yz|p_y|\delta_{3l}^-\rangle|^2}{E_{\Gamma_{25}^+}-E_{\Gamma_{15}^-}}, \tag{3.24}$$

where $\delta_{3l}^- \in \Gamma_{15}^-$. There are no matrix elements with δ_{1l}^- and δ_{2l}^-, where $\delta_{1l}^-, \delta_{2l}^-, \delta_{3l}^- \sim x, y, z$:

$$\begin{aligned}\langle yz|p_y|y\rangle &\overset{IC_{2y}}{=} 0,\\ \langle yz|p_y|x\rangle &\overset{IC_{2z}}{=} 0,\end{aligned}$$

but

$$\langle yz|p_y|z\rangle \neq 0.$$

Similarly, let

$$H_2 \equiv \frac{\hbar^2}{m_0^2} \sum_l{}' \frac{|\langle yz|p_y|\varepsilon_{3l}^-\rangle|^2}{E_{\Gamma_{25}^+} - E_{\Gamma_{25}^-}}. \tag{3.25}$$

Let $\Gamma_{25}^- \sim d_a - d_a'$ [e.g., $(yz)_a - (yz)_a'$]; except for operations with inversion, the matrix elements behave as for Γ_{25}^+. Then

$$\langle yz^+|p_y|yz^-\rangle = 0,$$

using C_{2x} and

$$\langle yz^+|p_y|\varepsilon_{2l}^-\rangle = 0,$$

using C_{2y} but

$$\langle yz^+|p_y|xy^-\rangle \neq 0.$$

Thus,

$$M = H_1 + H_2. \tag{3.26}$$

3.2.3.3 *N* Parameter

Finally, we study N:

$$\begin{aligned} N &= \frac{\hbar^2}{m_0^2} \sum_{l\nu\alpha}{}' \frac{\langle yz|p_x|l\nu\alpha\rangle\langle l\nu\alpha|p_y|yz\rangle + \langle yz|p_y|l\nu\alpha\rangle\langle l\nu\alpha|p_x|yz\rangle}{E_{\Gamma_{25}^+} - E_l} \\ &\sim \Gamma_2^- + \Gamma_{12}^- + \Gamma_{15}^- + \Gamma_{25}^-. \end{aligned} \tag{3.27}$$

We will consider the two matrix elements $\langle yz|p_x|l\rangle\langle l|p_y|yz\rangle$ and $\langle yz|p_y|l\rangle\langle l|p_x|yz\rangle$ separately. For Γ_2^-, we have first the matrix element $\langle yz|p_x|\beta_l^-\rangle\langle\beta_l^-|p_y|yz\rangle$, where $\beta_l^- \sim xyz$. Now,

$$\begin{aligned} \langle\beta_l^-|p_y|yz\rangle &= \langle xyz|p_y|zx\rangle \overset{IC_{2x\bar{y}}}{=} \langle xyz|p_x|yz\rangle = \langle\beta_l^-|p_x|yz\rangle, \\ \langle yz|p_y|l\alpha\rangle &= \langle yz|p_y|xyz\rangle = 0. \end{aligned}$$

Hence,

$$\frac{\hbar^2}{m_0^2} \sum_{l\in\Gamma_2^-}{}' \frac{\langle yz|p_x|l\rangle\langle l|p_y|yz\rangle + \langle yz|p_y|l\rangle\langle l|p_x|yz\rangle}{E_{\Gamma_{25}^+} - E_l} = \frac{\hbar^2}{m_0^2} \sum_{l\in\Gamma_2^-}{}' \frac{|\langle yz|p_x|\beta_l^-\rangle|^2}{E_{\Gamma_{25}^+} - E_l} \equiv F. \tag{3.28}$$

For Γ_{12}^{-}, we need the following:

$$\begin{aligned}
\langle \gamma_2^- | p_y | yz \rangle &= \left\langle \left(x^2+\omega^2 y^2+\omega z^2\right)^- |p_y| zx \right\rangle \overset{C_{4z}(y\bar{x}z)}{=} -\left\langle \left(y^2+\omega^2 x^2+\omega z^2\right)^- |p_x| zy \right\rangle \\
&= -\frac{1}{\omega^*} \left\langle \left(x^2+\omega y^2+\omega^2 z^2\right)^- |p_x| yz \right\rangle = -\omega \langle \gamma_1^- | p_x | yz \rangle, \\
\langle \gamma_1^- | p_y | yz \rangle &= \frac{1}{\omega^2} \langle \gamma_2^- | p_x | yz \rangle = -\frac{R}{\omega^2} = -\omega R, \\
&= \left\langle \left(x^2+\omega y^2+\omega^2 z^2\right)^- |p_y| zx \right\rangle \overset{C_{2xz}(z\bar{y}x)}{=} -\left\langle \left(z^2+\omega y^2+\omega^2 x^2\right)^- |p_y| xz \right\rangle \\
&= -\frac{1}{\omega} \left\langle \left(x^2+\omega^2 y^2+\omega z^2\right)^- |p_y| zx \right\rangle = -\omega^2 \left\langle \gamma_2^- | p_y | yz \right\rangle, \\
\left\langle zx | p_y | \gamma_1^- \right\rangle &= \left\langle zx |p_y| \left(x^2+\omega y^2+\omega^2 z^2\right)^- \right\rangle \overset{IC_{2x\bar{y}}(yxz)}{=} -\left\langle zy |p_x| \left(y^2+\omega x^2+\omega^2 z^2\right)^- \right\rangle \\
&= -\frac{1}{\omega^2} \left\langle yz | p_x | (x^2+\omega^2 y^2+\omega z^2)^- \right\rangle = -\frac{1}{\omega^2} \langle yz | p_x | \gamma_2^- \rangle,
\end{aligned}$$

or

$$\begin{aligned}
\left\langle yz | p_x | \gamma_2^- \right\rangle &= R = \left\langle yz | p_x | \gamma_1^- \right\rangle, \\
\langle \gamma_2^- | p_y | yz \rangle &= \frac{1}{\omega} \left\langle \gamma_1^- | p_x | yz \right\rangle, \\
\Longrightarrow \quad \langle yz | p_x | \gamma_2^- \rangle \langle \gamma_2^- | p_y | yz \rangle &= \frac{1}{\omega} \langle yz | p_x | \gamma_1^- \rangle \langle \gamma_1^- | p_x | yz \rangle = \frac{1}{\omega} |R|^2.
\end{aligned}$$

Next

$$\langle yz | p_x | \gamma_1^- \rangle \langle \gamma_1^- | p_y | yz \rangle = \langle yz | p_x | \gamma_2^- \rangle \frac{1}{\omega^2} \langle \gamma_2^- | p_x | yz \rangle = \frac{1}{\omega^2} |\langle yz | p_x | \gamma_2^- \rangle|^2 = \frac{1}{\omega^2} |R|^2.$$

Finally, in $\langle yz | p_y | l \rangle \langle l | p_x | yz \rangle$, e.g.,

$$\langle yz | p_y | (x^2+\omega y^2+\omega^2 z^2)^- \rangle \overset{C_{2y}}{=} 0.$$

Hence,

$$\begin{aligned}
&\frac{\hbar^2}{m_0^2} \sum_\nu \frac{\langle yz | p_x | \gamma_\nu^- \rangle \langle \gamma_\nu^- | p_y | yz \rangle}{E_{\Gamma_{25}^+} - E_l} \\
&= \frac{\hbar^2}{m_0^2} \left(\frac{1}{\omega} + \frac{1}{\omega^2} \right) \sum_\nu \frac{|R|^2}{E_{\Gamma_{25}^+} - E_l} = (\omega^2+\omega) \frac{\hbar^2}{m_0^2} \sum_\nu \frac{|R|^2}{E_{\Gamma_{25}^+} - E_l} = -\frac{\hbar^2}{m_0^2} \sum_\nu \frac{|R|^2}{E_{\Gamma_{25}^+} - E_l} \\
&\equiv -G.
\end{aligned}$$

For $\Gamma_{15}^{-} \sim x, y, z$, we have

$$\begin{aligned}\langle yz|p_x|\delta_{\nu l}^{-}\rangle\langle\delta_{\nu l}^{-}|p_y|yz\rangle &= \langle yz|p_x|x,y,z\rangle\langle x,y,z|p_y|zx\rangle = 0\ \forall\ \nu,\\ \langle yz|p_y|\delta_{\nu l}^{-}\rangle\langle\delta_{\nu l}^{-}|p_x|yz\rangle &= \langle yz|p_y|z\rangle\langle z|p_x|zx\rangle \neq 0.\end{aligned}$$

Indeed,

$$\begin{aligned}\langle yz|p_x|z\rangle &= \langle yx|p_y|x\rangle = \langle xy|p_y|\delta_{1l}^{-}\rangle,\\ \langle z|p_y|zx\rangle &= \langle x|p_y|xy\rangle = \langle\delta_{1l}^{-}|p_y|xy\rangle,\end{aligned}$$

giving

$$\sum_{\Gamma_{15}^{-}} = H_1. \tag{3.29}$$

For $\Gamma_{25}^{-} \sim d_a - d_a'$, we have

$$\langle yz|p_x|\varepsilon_{\nu l}^{-}\rangle\langle\varepsilon_{\nu l}^{-}|p_y|zx\rangle = 0.$$

We already have that

$$\langle yz|p_y|\varepsilon_{1,2l}^{-}\rangle = 0.$$

Thus, the only non-zero element is

$$\langle yz|p_y|\varepsilon_{3l}^{-}\rangle\langle\varepsilon_{3l}^{-}|p_x|zx\rangle \overset{C_{4z}}{=} -\langle yz|p_y|xy^{-}\rangle\langle xy^{-}|p_y|yz\rangle = -H_2.$$

Finally,

$$N = F - G + H_1 - H_2. \tag{3.30}$$

3.2.4 Properties

Rewriting the DKK Hamiltonian, Eq. (3.4), as

$$Mk^2 + \begin{pmatrix} (L-M)k_x^2 & Nk_xk_y & Nk_xk_z \\ Nk_xk_y & (L-M)k_y^2 & Nk_yk_z \\ Nk_xk_z & Nk_yk_z & (L-M)k_z^2 \end{pmatrix},$$

one observes that if $(L - M) = N$, the energy dispersion is isotropic. This is known as the spherical approximation; it was first introduced by Baldereschi and Lipari in their study of acceptor states in cubic semiconductors [30].

Note that a minimal basis (sp^3) tight-binding model will give an isotropic dispersion for small wave vector [24]. In this respect, $k \cdot p$ theory gives a better representation of the symmetry group (if enough interactions are retained). Indeed, if one only retains the lowest interaction (assumed to be of symmetry $\Gamma_2^- \sim xyz$), and defines a Kane parameter analogously to the ZB case [Eq. (2.30)],

$$\frac{2}{m_0}|\langle xyz|p_z|xy\rangle|^2 \equiv E_P,$$

then

$$\begin{aligned} L &= \frac{\hbar^2}{m_0^2}\frac{|\langle xy|p_z|xyz\rangle|^2}{E_{\Gamma_{25}^+} - E_2^-} = \frac{\hbar^2}{2m_0}\left(\frac{E_P}{-E_0}\right), \\ M &= 0, \\ N &= L, \end{aligned}$$

giving an isotropic dispersion (and effective mass).

Table 3.3 DKK parameters in units of $\hbar^2/2m_0$ [2]

	L	M	N	F	G	H_1	H_2
Si	−1.9	−6.7	−7.5	−1.2	−0.4	−6.7	0
Ge	−31.8	−5.1	−32.1	−28.6	−1.4	−5.1	0

The band structures for Si and Ge along $L \to \Gamma \to X$ are plotted in Fig. 3.3, using the parameters from Table 3.3. H_2 was chosen zero since it involves interaction with Γ_{25}^- states and those are far from the valence band (Fig. 3.2). The warping is evident from the difference in dispersion along the two directions. Also, the significant failure of the $k \cdot p$ for large k is evident in the unnaturally large bandwidths.

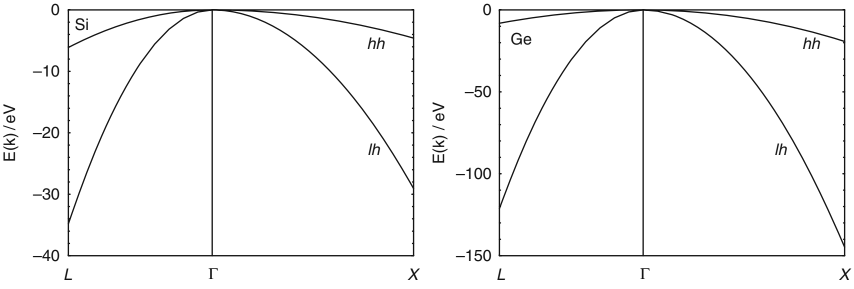

Fig. 3.3 Si and Ge band structures from DKK model

3.3 Six-Band Model for Diamond

We now add the spin-orbit coupling to the previous model.

3.3.1 Hamiltonian

First we recall that the $k \cdot p$ perturbation was present to second order. However, the spin-orbit interaction is nonzero even to first order. There are two contributions in the $k \cdot p$ equation:

$$H_{\mathrm{so}}(\mathbf{k}) = \frac{\hbar}{4m_0^2c^2}(\boldsymbol{\sigma} \times \nabla V) \cdot \mathbf{p} + \frac{\hbar^2}{4m_0^2c^2}(\boldsymbol{\sigma} \times \nabla V) \cdot \mathbf{k} = H_{\mathrm{so}} + H_{\mathrm{so},k}. \tag{3.31}$$

The second, k-dependent spin-orbit term is usually much smaller than the first one [3]; we will ignore it for now. Hence, we will be adding the matrix elements of H_{so} in the Γ_{25}^+ subspace and we rewrite the first term of Eq. (3.31) as

$$H_{\mathrm{so}} = \frac{\hbar}{4m_0^2c^2}(\boldsymbol{\sigma} \times \nabla V) \cdot \mathbf{p} = \frac{\hbar}{4m_0^2c^2}(\nabla V \times \mathbf{p}) \cdot \boldsymbol{\sigma} \equiv H_{\mathrm{s},i}\sigma_i. \tag{3.32}$$

One can show that there exists only one independent spin-orbit matrix element since $\nabla V \times \mathbf{p}$ is an axial vector. Then

$$\langle s|\nabla V \times \mathbf{p}|x\rangle = \langle x|\nabla V \times \mathbf{p}|x\rangle = 0,$$

and

$$\langle x|(\nabla V \times \mathbf{p})_z|y\rangle \neq 0.$$

Historically, one writes

$$\Delta_0 \equiv \frac{3\mathrm{i}\hbar}{4m_0^2c^2}\left\langle x\left|\frac{\partial V}{\partial x}p_y - \frac{\partial V}{\partial y}p_x\right|y\right\rangle. \tag{3.33}$$

Kane [31] wrote it differently, as

$$\Delta \equiv -\frac{3\mathrm{i}\hbar}{4m_0^2c^2}\langle x|(\nabla V \times \mathbf{p})_y|z\rangle,$$

but one can show both forms lead to equivalent H_{so} matrices.

It is necessary to include the spin functions to the basis states leading to a six-dimensional basis: $\varepsilon_1^+ \uparrow$, $\varepsilon_2^+ \uparrow$, $\varepsilon_3^+ \uparrow$, $\varepsilon_1^+ \downarrow$, $\varepsilon_2^+ \downarrow$, $\varepsilon_3^+ \downarrow$. In this LS representation, H_{so} is not diagonal. Equivalently, it mixes the states and can lead to a splitting of the degeneracy. Indeed, the six states transform according to (Table B.6)

$$\Gamma_{25}^+ \otimes \Gamma_6^+ = \Gamma_8^+ \oplus \Gamma_7^+,$$

and split into a quadruplet and a doublet. The double-group notation is that of Dresselhaus [32] as opposed to that of Koster et al. [33].

However, if one transforms to the JM_J basis, H_{so} is diagonal. That this is so can be seen from the fact that H_{so} behaves as

$$\mathbf{L}\cdot\mathbf{S} = \frac{1}{2}(J^2 - L^2 - S^2) = \frac{1}{2}\left[j(j+1) - l(l+1) - s(s+1)\right].$$

Combining the p-like orbitals ($l = 1$) with the spinors ($s = \frac{1}{2}$) leads to $j = \frac{3}{2}$ (four-fold degenerate) or $j = \frac{1}{2}$ (two-fold degenerate) states. We choose phases following Bastard [7] (Table 3.4). Our next task is to transform the Hamiltonian into the new JM_J basis and then attempt to find exact solutions. We do expect, from Kramer's degeneracy, that all the states will be doubly degenerate.

Table 3.4 $|J\ M_J\rangle$ states. The phase factors given agree with, e.g., Bastard [7] and Foreman [34]

$$\begin{aligned}
\left|\frac{3}{2}\ \frac{3}{2}\right\rangle &= \frac{1}{\sqrt{2}}|(x+\mathrm{i}y)\uparrow\rangle,\\
\left|\frac{3}{2}\ \frac{1}{2}\right\rangle &= \frac{1}{\sqrt{6}}|(x+\mathrm{i}y)\downarrow\rangle - \sqrt{\frac{2}{3}}|z\uparrow\rangle,\\
\left|\frac{3}{2}\ {-\frac{1}{2}}\right\rangle &= -\frac{1}{\sqrt{6}}|(x-\mathrm{i}y)\uparrow\rangle - \sqrt{\frac{2}{3}}|z\downarrow\rangle,\\
\left|\frac{3}{2}\ {-\frac{3}{2}}\right\rangle &= \frac{1}{\sqrt{2}}|(x-\mathrm{i}y)\downarrow\rangle,\\
\left|\frac{1}{2}\ \frac{1}{2}\right\rangle &= \frac{1}{\sqrt{3}}|(x+\mathrm{i}y)\downarrow\rangle + \frac{1}{\sqrt{3}}|z\uparrow\rangle,\\
\left|\frac{1}{2}\ {-\frac{1}{2}}\right\rangle &= -\frac{1}{\sqrt{3}}|(x-\mathrm{i}y)\uparrow\rangle + \frac{1}{\sqrt{3}}|z\downarrow\rangle,\\
&\mathrm{i}|s\uparrow\rangle,\\
&\mathrm{i}|s\downarrow\rangle.
\end{aligned}$$

3.3.1.1 H_{so}

Consider first the spin-orbit term. We need the Pauli spin matrices:

$$\sigma_x = \begin{pmatrix}0 & 1\\ 1 & 0\end{pmatrix}, \sigma_y = \begin{pmatrix}0 & -\mathrm{i}\\ \mathrm{i} & 0\end{pmatrix}, \sigma_z = \begin{pmatrix}1 & 0\\ 0 & -1\end{pmatrix}. \tag{3.34}$$

In the JM_J basis, H_{so} is diagonal; furthermore, the matrix elements are only dependent upon J. For example,

$$\begin{aligned}
\left\langle\frac{3}{2}\ \frac{3}{2}\right|H_{\text{so}}\left|\frac{3}{2}\ \frac{3}{2}\right\rangle &= \left\langle\frac{3}{2}\ \frac{3}{2}\right|\left|\frac{\hbar}{4m_0^2c^2}\right|(\nabla V\times\mathbf{p})\cdot\boldsymbol{\sigma}\left|\frac{3}{2}\ \frac{3}{2}\right\rangle\\
&= \frac{1}{2}\langle(x+\mathrm{i}y)\uparrow|\frac{\hbar}{4m_0^2c^2}(\nabla V\times\mathbf{p})\cdot\boldsymbol{\sigma}|(x+\mathrm{i}y)\uparrow\rangle
\end{aligned}$$

$$
\begin{aligned}
&= \frac{1}{2}\langle (x+\mathrm{i}y)|\frac{\hbar}{4m_0^2c^2}(\nabla V \times \mathbf{p})|(x+\mathrm{i}y)\rangle \cdot \langle\uparrow|\boldsymbol{\sigma}|\uparrow\rangle \\
&= \mathrm{i}\langle x|\frac{\hbar}{4m_0^2c^2}(\nabla V \times \mathbf{p})|y\rangle \cdot \langle\uparrow|\boldsymbol{\sigma}|\uparrow\rangle \\
&= \mathrm{i}\langle x|\frac{\hbar}{4m_0^2c^2}(\nabla V \times \mathbf{p})_z|y\rangle \equiv \frac{\Delta_0}{3}, \qquad (3.35)
\end{aligned}
$$

using Eq. (3.33). Similarly, one finds

$$
\left\langle \frac{1}{2}\,\frac{1}{2}|H_{\mathrm{so}}|\frac{1}{2}\,\frac{1}{2}\right\rangle = -\frac{2\Delta_0}{3}.
$$

A more formal procedure is to transform H_{so} in LS to H'_{so} in JM_J. In LS, we have

$$
H_{\mathrm{so}} = \frac{1}{3}\Delta_0 \left(\begin{array}{cccccc}
\varepsilon_1^+\uparrow & \varepsilon_2^+\uparrow & \varepsilon_3^+\uparrow & \varepsilon_1^+\downarrow & \varepsilon_2^+\downarrow & \varepsilon_3^+\downarrow \\
0 & -\mathrm{i} & 0 & 0 & 0 & 1 \\
\mathrm{i} & 0 & 0 & 0 & 0 & -\mathrm{i} \\
0 & 0 & 0 & -1 & \mathrm{i} & 0 \\
0 & 0 & -1 & 0 & \mathrm{i} & 0 \\
0 & 0 & -\mathrm{i} & -\mathrm{i} & 0 & 0 \\
1 & \mathrm{i} & 0 & 0 & 0 & 0
\end{array}\right). \qquad (3.36)
$$

We now need the transformation matrix S connecting the LS states to the JM_J ones. The equations in Table 3.4 can be rewritten in column vector form as

$$
|JM_J\rangle^T = S^T \cdot |LS\rangle^T, \qquad (3.37)
$$

or in row vector form

$$
\langle JM_J| = \langle LS| \cdot S, \qquad (3.38)
$$

which defines the matrix S as

$$
S = \left(\begin{array}{ccccccc}
 & |\frac{3}{2}\,\frac{3}{2}\rangle & |\frac{3}{2}\,\frac{1}{2}\rangle & |\frac{3}{2}\,-\frac{1}{2}\rangle & |\frac{3}{2}\,-\frac{3}{2}\rangle & |\frac{1}{2}\,\frac{1}{2}\rangle & |\frac{1}{2}\,-\frac{1}{2}\rangle \\
|\varepsilon_1^+\uparrow\rangle & \frac{1}{\sqrt{2}} & 0 & -\frac{1}{\sqrt{6}} & 0 & 0 & -\frac{1}{\sqrt{3}} \\
|\varepsilon_2^+\uparrow\rangle & \frac{\mathrm{i}}{\sqrt{2}} & 0 & \frac{\mathrm{i}}{\sqrt{6}} & 0 & 0 & \frac{\mathrm{i}}{\sqrt{3}} \\
|\varepsilon_3^+\uparrow\rangle & 0 & -\sqrt{\frac{2}{3}} & 0 & 0 & \sqrt{\frac{1}{3}} & 0 \\
|\varepsilon_1^+\downarrow\rangle & 0 & \frac{1}{\sqrt{6}} & 0 & \frac{1}{\sqrt{2}} & \frac{1}{\sqrt{3}} & 0 \\
|\varepsilon_2^+\downarrow\rangle & 0 & \frac{\mathrm{i}}{\sqrt{6}} & 0 & -\frac{\mathrm{i}}{\sqrt{2}} & \frac{\mathrm{i}}{\sqrt{3}} & 0 \\
|\varepsilon_3^+\downarrow\rangle & 0 & 0 & -\sqrt{\frac{2}{3}} & 0 & 0 & \sqrt{\frac{1}{3}}
\end{array}\right). \qquad (3.39)
$$

Note that this differs from Eq. (10) of Kane [3] in an overall sign and also in a different ordering of the JM_J basis. We can state that his $|JM_J\rangle$ states differ from ours by an overall sign (Table C.2). The spin-orbit Hamiltonian in the JM_J basis is

$$H'_{\text{so}} = S^\dagger H_{\text{so}} S = \frac{\Delta_0}{3}\begin{pmatrix} 1 & 0 & 0 & 0 & 0 & 0 \\ 0 & 1 & 0 & 0 & 0 & 0 \\ 0 & 0 & 1 & 0 & 0 & 0 \\ 0 & 0 & 0 & 1 & 0 & 0 \\ 0 & 0 & 0 & 0 & -2 & 0 \\ 0 & 0 & 0 & 0 & 0 & -2 \end{pmatrix}. \tag{3.40}$$

3.3.1.2 $H_{k\cdot p}$

We now consider the representation of the $k \cdot p$ perturbation in the JM_J basis:

$$H_{rs} = \sum_{l\alpha} \frac{\langle r|H_{k\cdot p}|l\alpha\rangle\langle l\alpha|H_{k\cdot p}|s\rangle}{E_0 - E_{l\alpha}}. \tag{3.41}$$

In principle, one would need to transform all the states. In Eq. (3.41), the combination $|l\alpha\rangle\langle l\alpha|$ is invariant under a unitary transformation; hence, they can be left unchanged. Their energies $E_{l\alpha}$ would, in general, experience spin-orbit splittings. Following DKK, we will neglect the latter effect. The Hamiltonian in the LS basis is

$$\begin{pmatrix} H_{\text{DKK}} & 0 \\ 0 & H_{\text{DKK}} \end{pmatrix}.$$

One can now obtain the Hamiltonian in the JM_J basis by performing a unitary transformation

$$S^{-1} H(\mathbf{k}) S,$$

The small size of the Hamiltonian together with hermiticity makes the direct transformation to the JM_J basis fairly straightforward. Furthermore, if left in terms of the matrix elements H_{ij} of H_{DKK}, the result reflects the choice of Clebsch-Gordan coefficients, i.e., the latter (together with hermiticity) govern the structure of the matrix. For example,

$$\begin{aligned}\left\langle \frac{3}{2}\ \frac{3}{2}|H(\mathbf{k})|\frac{3}{2}\ \frac{3}{2}\right\rangle &= \frac{1}{2}\langle (x+\mathrm{i}y)\uparrow |H(\mathbf{k})|(x+\mathrm{i}y)\uparrow\rangle \\ &= \frac{1}{2}(H_{11}+H_{22}) = \left\langle \frac{3}{2}\ -\frac{3}{2}|H(\mathbf{k})|\frac{3}{2}\ -\frac{3}{2}\right\rangle \equiv P',\end{aligned}$$

$$\left\langle \frac{3}{2}\ \frac{1}{2}|H(\mathbf{k})|\frac{3}{2}\ \frac{1}{2}\right\rangle = \left\langle \frac{1}{\sqrt{6}}(x+\mathrm{i}y)\downarrow -\sqrt{\frac{2}{3}}z\uparrow |H(\mathbf{k})|\frac{1}{\sqrt{6}}(x+\mathrm{i}y)\downarrow -\sqrt{\frac{2}{3}}z\uparrow\right\rangle$$

$$
\begin{aligned}
&= \frac{1}{6}\langle x+\mathrm{i}y|H(\mathbf{k})|x+\mathrm{i}y\rangle + \frac{2}{3}\langle z|H(\mathbf{k})|z\rangle \\
&= \frac{1}{6}(H_{11}+H_{22}) + \frac{2}{3}H_{33} = \left\langle \frac{3}{2}\ -\frac{1}{2}|H(\mathbf{k})|\frac{3}{2}\ -\frac{1}{2}\right\rangle \equiv P'',
\end{aligned}
$$

$$
\begin{aligned}
\left\langle \frac{1}{2}\ \frac{1}{2}|H(\mathbf{k})|\frac{1}{2}\ \frac{1}{2}\right\rangle &= \left\langle \frac{1}{\sqrt{3}}(x+\mathrm{i}y)\downarrow + \frac{1}{\sqrt{3}}z\uparrow |H(\mathbf{k})| \frac{1}{\sqrt{3}}(x+\mathrm{i}y)\downarrow + \frac{1}{\sqrt{3}}z\uparrow \right\rangle \\
&= \frac{1}{3}\langle x+\mathrm{i}y|H(\mathbf{k})|x+\mathrm{i}y\rangle + \frac{1}{3}\langle z|H(\mathbf{k})|z\rangle \\
&= \frac{1}{3}(H_{11}+H_{22}+H_{33}) = \left\langle \frac{1}{2}\ -\frac{1}{2}|H(\mathbf{k})|\frac{1}{2}\ -\frac{1}{2}\right\rangle \equiv P''',
\end{aligned}
$$

$$
\begin{aligned}
\left\langle \frac{3}{2}\ \frac{3}{2}|H(\mathbf{k})|\frac{3}{2}\ \frac{1}{2}\right\rangle &= \left\langle \frac{1}{\sqrt{2}}(x+\mathrm{i}y)\uparrow |H(\mathbf{k})| \frac{1}{\sqrt{6}}(x+\mathrm{i}y)\downarrow - \sqrt{\frac{2}{3}}z\uparrow \right\rangle \\
&= -\frac{1}{\sqrt{3}}\langle x+\mathrm{i}y|H(\mathbf{k})|z\rangle = -\frac{1}{\sqrt{3}}(H_{13}-\mathrm{i}H_{23}) \equiv S_-,
\end{aligned}
$$

$$
\begin{aligned}
\left\langle \frac{3}{2}\ \frac{3}{2}|H(\mathbf{k})|\frac{3}{2}\ -\frac{1}{2}\right\rangle &= \left\langle \frac{1}{\sqrt{2}}(x+\mathrm{i}y)\uparrow |H(\mathbf{k})| -\frac{1}{\sqrt{6}}(x+\mathrm{i}y)\uparrow - \sqrt{\frac{2}{3}}z\downarrow \right\rangle \\
&= -\frac{1}{2\sqrt{3}}\langle x+\mathrm{i}y|H(\mathbf{k})|x-\mathrm{i}y\rangle = -\frac{1}{2\sqrt{3}}(H_{11}-H_{22}-2\mathrm{i}H_{12}) \\
&\equiv -R,
\end{aligned}
$$

$$
\begin{aligned}
\left\langle \frac{3}{2}\ \frac{1}{2}|H(\mathbf{k})|\frac{1}{2}\ \frac{1}{2}\right\rangle &= \left\langle \frac{1}{\sqrt{6}}(x+\mathrm{i}y)\downarrow - \sqrt{\frac{2}{3}}z\uparrow |H(\mathbf{k})| \frac{1}{\sqrt{3}}(x+\mathrm{i}y)\downarrow + \frac{1}{\sqrt{3}}z\uparrow \right\rangle \\
&= \frac{1}{3\sqrt{2}}\langle x+\mathrm{i}y|H(\mathbf{k})|x+\mathrm{i}y\rangle - \frac{\sqrt{2}}{3}\langle z|H(\mathbf{k})|z\rangle \\
&= \frac{1}{3\sqrt{2}}(H_{11}+H_{22}-2H_{33}) \equiv -\sqrt{2}Q,
\end{aligned}
$$

$$
\begin{aligned}
\left\langle \frac{3}{2}\ -\frac{1}{2}|H(\mathbf{k})|\frac{1}{2}\ \frac{1}{2}\right\rangle &= -\frac{1}{3\sqrt{2}}\langle x-\mathrm{i}y|H(\mathbf{k})|z\rangle - \frac{\sqrt{2}}{3}\langle z|H(\mathbf{k})|x+\mathrm{i}y\rangle \\
&= -\frac{1}{\sqrt{2}}(H_{13}+\mathrm{i}H_{23}) = \sqrt{\frac{3}{2}}S_+.
\end{aligned}
$$

In the above derivations, we have used the fact that $H_{ij} = H_{ji}$.

3.3.1.3 $H(\mathbf{k}) + H_{\mathrm{so}}$

The total Hamiltonian is given in Table 3.5. Note that there are a few sign differences between our Table 3.5 and Eq. (65) of DKK. These can be accounted for by differences in the phases of two of the basis functions (Table C.2), even though DKK did not give theirs explicitly. For example, in our case, the (1,5) and (2,6) matrix elements have the same sign; in DKK's case, they have opposite signs. Equation (4.3.14) in S. L. Chuang's book [15] (and Eq. (20) of Elliott [35] but there are other problems here as we will see below) also have the same structure as DKK's; in the former case, the basis functions are given and the sign difference in two basis functions is consistent with our interpretation of DKK's basis. Our Hamiltonian has the same structure as that of, e.g., Kane [3] (not surprisingly since our bases only differ by an overall negative sign) and, in fact, of Luttinger–Kohn [6] as well, as we will see later for both cases. Nevertheless, the subsequent evaluation of the secular determinant leads to the same characteristic equation. Our Hamiltonian does agree with that of Kane [3] upon re-ordering the basis. Before we treat the approximate eigenvalues, we give here the explicit and independent matrix elements of the 6 × 6 Hamiltonian given in Table 3.5, using the notation of Elliot [35]:

$$
\begin{aligned}
(1,1) = (4,4) &= \frac{H_{11}+H_{22}}{2} = \frac{1}{2}(L+M)(k_x^2+k_y^2) + Mk_z^2 \equiv \frac{1}{2}P - \frac{\hbar^2k^2}{2m_0},\\
(1,2) &= -\frac{H_{13}-\mathrm{i}H_{23}}{\sqrt{3}} = -\frac{N}{\sqrt{3}}(k_x-\mathrm{i}k_y)k_z \equiv R,\\
(1,3) &= -\frac{H_{11}-H_{22}-2\mathrm{i}H_{12}}{2\sqrt{3}} = -\frac{1}{2\sqrt{3}}\left[(L-M)(k_x^2-k_y^2) - 2\mathrm{i}Nk_xk_y\right] \equiv S,\\
(2,2) = (3,3) &= \frac{H_{11}+H_{22}+4H_{33}}{6} = \frac{1}{6}\left[(L+5M)(k_x^2+k_y^2) + 2(2L+M)k_z^2\right]\\
&\equiv \frac{1}{6}P + \frac{2}{3}Q - \frac{\hbar^2k^2}{2m_0},\\
(2,5) &= \frac{H_{11}+H_{22}-2H_{33}}{3\sqrt{2}} = \frac{1}{3\sqrt{2}}\left[(L-M)(k_x^2+k_y^2) - 2(L-M)k_z^2\right]\\
&\equiv \frac{1}{3\sqrt{2}}(P-2Q),\\
(5,5) = (6,6) &= \frac{H_{11}+H_{22}+H_{33}}{3} - \Delta_0 = \frac{L+2M}{3}k^2 - \Delta_0\\
&\equiv \frac{1}{3}(P+Q) - \Delta_0 - \frac{\hbar^2k^2}{2m_0}.
\end{aligned}
$$

The above can be summarized into the Elliott–Luttinger–Kohn Hamiltonian in Table 3.6, after adding the diagonal free-electron energy term. Note, however, that our matrix differs slightly from the original Elliott [35] and LK [6] ones due to the different basis functions used. Indeed, if we correct for the difference in basis function, we do reproduce the LK Hamiltonian, Eq. (V.13); but we do not reproduce that of Elliott. Our P and Q are identical to the latter but not R and S. Since we have already used L, M, N as DKK parameters, we have introduced a new notation to replace the k-dependent L, M of LK; we, henceforth, refer to the LK k-dependent matrix elements as P_L, Q_L, L_L, M_L. The relationships between ours and LK's are:

Table 3.5 DKK Hamiltonian in JM_J basis. The top matrix is as given by DKK [2], the second emphasizes the structure due solely to the Clebsch-Gordan coefficients and hermiticity (thus the lower half of the matrix is not explicitly written out). H_{ij} are matrix elements of H_{DKK}

$$\left(\begin{array}{cccccc}
|\frac{3}{2}\ \frac{3}{2}\rangle & |\frac{3}{2}\ \frac{1}{2}\rangle & |\frac{3}{2}\ -\frac{1}{2}\rangle & |\frac{3}{2}\ -\frac{3}{2}\rangle & |\frac{1}{2}\ \frac{1}{2}\rangle & |\frac{1}{2}\ -\frac{1}{2}\rangle \\
\frac{H_{11}+H_{22}}{2} & -\frac{H_{13}-\mathrm{i}H_{23}}{\sqrt{3}} & -\frac{H_{11}-H_{22}-2\mathrm{i}H_{12}}{2\sqrt{3}} & 0 & \frac{H_{13}-\mathrm{i}H_{23}}{\sqrt{6}} & -\frac{H_{11}-H_{22}-2\mathrm{i}H_{12}}{\sqrt{6}} \\
-\frac{H_{13}+\mathrm{i}H_{23}}{\sqrt{3}} & \frac{4H_{33}+H_{11}+H_{22}}{6} & 0 & \frac{H_{11}-H_{22}-2\mathrm{i}H_{12}}{2\sqrt{3}} & \frac{H_{11}+H_{22}-2H_{33}}{3\sqrt{2}} & \frac{H_{13}-\mathrm{i}H_{23}}{\sqrt{2}} \\
-\frac{H_{11}-H_{22}+2\mathrm{i}H_{12}}{2\sqrt{3}} & 0 & \frac{4H_{33}+H_{11}+H_{22}}{6} & -\frac{H_{13}-\mathrm{i}H_{23}}{\sqrt{3}} & -\frac{H_{13}+\mathrm{i}H_{23}}{\sqrt{2}} & \frac{H_{11}+H_{22}-2H_{33}}{3\sqrt{2}} \\
0 & \frac{H_{11}-H_{22}+2\mathrm{i}H_{12}}{2\sqrt{3}} & -\frac{H_{13}+\mathrm{i}H_{23}}{\sqrt{3}} & \frac{H_{11}+H_{22}}{2} & \frac{H_{11}-H_{22}+2\mathrm{i}H_{12}}{\sqrt{6}} & \frac{H_{13}+\mathrm{i}H_{23}}{\sqrt{6}} \\
\frac{H_{13}+\mathrm{i}H_{23}}{\sqrt{6}} & \frac{H_{11}+H_{22}-2H_{33}}{3\sqrt{2}} & -\frac{H_{13}-\mathrm{i}H_{23}}{\sqrt{2}} & \frac{H_{11}-H_{22}-2\mathrm{i}H_{12}}{\sqrt{6}} & \frac{H_{11}+H_{22}+H_{33}}{3}-\Delta_0 & 0 \\
-\frac{H_{11}-H_{22}+2\mathrm{i}H_{12}}{\sqrt{6}} & \frac{H_{13}+\mathrm{i}H_{23}}{\sqrt{2}} & \frac{H_{11}+H_{22}-2H_{33}}{3\sqrt{2}} & \frac{H_{13}-\mathrm{i}H_{23}}{\sqrt{6}} & 0 & \frac{H_{11}+H_{22}+H_{33}}{3}-\Delta_0
\end{array}\right)$$

$$\equiv \left(\begin{array}{cccccc}
|\frac{3}{2}\ \frac{3}{2}\rangle & |\frac{3}{2}\ \frac{1}{2}\rangle & |\frac{3}{2}\ -\frac{1}{2}\rangle & |\frac{3}{2}\ -\frac{3}{2}\rangle & |\frac{1}{2}\ \frac{1}{2}\rangle & |\frac{1}{2}\ -\frac{1}{2}\rangle \\
P' & S_- & -R & 0 & -\frac{1}{\sqrt{2}}S_- & -\sqrt{2}R \\
 & P'' & 0 & R & -\sqrt{2}Q & -\sqrt{\frac{3}{2}}S_- \\
 & & P'' & S_- & \sqrt{\frac{3}{2}}S_+ & -\sqrt{2}Q \\
 & \dagger & & P' & \sqrt{2}R^* & \frac{1}{\sqrt{2}}S_+ \\
 & & & & P''' - \Delta_0 & 0 \\
 & & & & & P''' - \Delta_0
\end{array}\right)$$

Table 3.6 DKK Hamiltonian in JM_J basis using Elliott-LK notation. Note differences compared to Eq. (20) of Elliott and Eq. (V.13) of LK. The free-electron energy was added to the DKK Hamiltonian

$$\left(\begin{array}{cccccc}
|\frac{3}{2}\ \frac{3}{2}\rangle & |\frac{3}{2}\ \frac{1}{2}\rangle & |\frac{3}{2}\ -\frac{1}{2}\rangle & |\frac{3}{2}\ -\frac{3}{2}\rangle & |\frac{1}{2}\ \frac{1}{2}\rangle & |\frac{1}{2}\ -\frac{1}{2}\rangle \\
\frac{1}{2}P & R & S & 0 & -\frac{1}{\sqrt{2}}R & \sqrt{2}S \\
R^* & \frac{1}{6}P+\frac{2}{3}Q & 0 & -S & \frac{1}{3\sqrt{2}}(P-2Q) & -\sqrt{\frac{3}{2}}R \\
S^* & 0 & \frac{1}{6}P+\frac{2}{3}Q & R & \sqrt{\frac{3}{2}}R^* & \frac{1}{3\sqrt{2}}(P-2Q) \\
0 & -S^* & R^* & \frac{1}{2}P & -\sqrt{2}S^* & -\frac{1}{\sqrt{2}}R^* \\
-\frac{1}{\sqrt{2}}R^* & \frac{1}{3\sqrt{2}}(P-2Q) & \sqrt{\frac{3}{2}}R & -\sqrt{2}S & \frac{1}{3}(P+Q)-\Delta_0 & 0 \\
\sqrt{2}S^* & -\sqrt{\frac{3}{2}}R^* & \frac{1}{3\sqrt{2}}(P-2Q) & -\frac{1}{\sqrt{2}}R & 0 & \frac{1}{3}(P+Q)-\Delta_0
\end{array}\right)$$

with

$$\begin{aligned}
P &= (L+M)(k_x^2+k_y^2)+2Mk_z^2+\frac{\hbar^2k^2}{m_0},\\
Q &= M(k_x^2+k_y^2)+Lk_z^2+\frac{\hbar^2k^2}{2m_0},\\
R &= -\frac{N}{\sqrt{3}}(k_x-\mathrm{i}k_y)k_z,\\
S &= -\frac{1}{2\sqrt{3}}\left[(L-M)(k_x^2-k_y^2)-2\mathrm{i}Nk_xk_y\right].
\end{aligned}$$

$$\begin{aligned}
P &= (L+M)(k_x^2+k_y^2)+2Mk_z^2+\frac{\hbar^2k^2}{m_0} = (A_L+B_L)(k_x^2+k_y^2)+2B_Lk_z^2 \equiv P_L,\\
Q &= M(k_x^2+k_y^2)+Lk_z^2+\frac{\hbar^2k^2}{2m_0} = Q_L,\\
R &= -\frac{N}{\sqrt{3}}(k_x-\mathrm{i}k_y)k_z = -\mathrm{i}L_L,\\
S &= -\frac{1}{2\sqrt{3}}\left[(L-M)(k_x^2-k_y^2)-2\mathrm{i}Nk_xk_y\right] = -M_L.
\end{aligned} \tag{3.42}$$

This form of the Hamiltonian is not widely used; exceptions include, e.g., in the paper by Sercel and Vahala [36].

While this Hamiltonian is often called the Luttinger–Kohn Hamiltonian, we note that it appears to have first been written down by Elliott in a related form [35]. There is also another form of this same Hamiltonian, e.g., in S. L. Chuang's book [15], in terms of the Luttinger parameters. However, since we have not yet introduced the Luttinger parameters, we will present this other form later. Note further that the quantities P, Q, R, S are different from the definitions in our canonical form in Table 3.5.

3.3.2 DKK Solution

The full 6 × 6 determinant cannot be solved analytically. If one assumes that the *hh*/*lh* states can be decoupled from the spin-split-off hole (*sh*) states (as they are for $\mathbf{k} = \mathbf{0}$), then one has a 2×2 and a 4×4 block. The spin-split-off block can obviously be diagonalized exactly. The 4 × 4 block, it turns out, can also be diagonalized exactly here due to the fact that all the states are doubly degenerate from time-reversal symmetry in an inversion-symmetric structure (Kramer's theorem).

We first obtain the spin-split-off dispersion. The 2×2 block is given by Eq. (3.43).

$$\begin{vmatrix} \frac{H_{11}+H_{22}+H_{33}}{3} - \lambda - \Delta_0 & 0 \\ 0 & \frac{H_{11}+H_{22}+H_{33}}{3} - \lambda - \Delta_0 \end{vmatrix} = 0. \tag{3.43}$$

Not surprisingly, the matrix is already diagonal, reflecting the double degeneracy expected. The eigenvalue is

$$\begin{aligned} \lambda &= -\Delta_0 + \frac{H_{11} + H_{22} + H_{33}}{3} \\ &= -\Delta_0 + \frac{1}{3}(L + 2M)k^2. \end{aligned}$$

The dispersion is

$$E_{sh}(\mathbf{k}) = \frac{\hbar^2 k^2}{2m_0} - \Delta_0 + \frac{1}{3}(L + 2M)k^2 \equiv -\Delta_0 + Ak^2, \tag{3.44}$$

where

$$A \equiv \frac{1}{3}(L + 2M) + \frac{\hbar^2}{2m_0}. \tag{3.45}$$

We now evaluate the 4 × 4 determinant in a straightforward manner:

$$\begin{vmatrix} \frac{H_{11}+H_{22}}{2} - \lambda & -\frac{H_{13}-\mathrm{i}H_{23}}{\sqrt{3}} & -\frac{H_{11}-H_{22}-2\mathrm{i}H_{12}}{2\sqrt{3}} & 0 \\ -\frac{H_{13}+\mathrm{i}H_{23}}{\sqrt{3}} & \frac{4H_{33}+H_{11}+H_{22}}{6} - \lambda & 0 & \frac{H_{11}-H_{22}-2\mathrm{i}H_{12}}{2\sqrt{3}} \\ -\frac{H_{11}-H_{22}+2\mathrm{i}H_{12}}{2\sqrt{3}} & 0 & \frac{4H_{33}+H_{11}+H_{22}}{6} - \lambda & -\frac{H_{13}-\mathrm{i}H_{23}}{\sqrt{3}} \\ 0 & \frac{H_{11}-H_{22}+2\mathrm{i}H_{12}}{2\sqrt{3}} & -\frac{H_{13}+\mathrm{i}H_{23}}{\sqrt{3}} & \frac{H_{11}+H_{22}}{2} - \lambda \end{vmatrix}$$

$$\begin{aligned} &= \left[\frac{1}{2}(H_{11} + H_{22}) - \lambda\right]^2 \left[\frac{1}{6}(4H_{33} + H_{11} + H_{22}) - \lambda\right]^2 \\ &\quad -\frac{1}{6}\left[\frac{1}{6}(4H_{33} + H_{11} + H_{22}) - \lambda\right]\left[\frac{1}{2}(H_{11} + H_{22}) - \lambda\right] \\ &\quad \times\left\{(H_{11} - H_{22})^2 + 4(H_{12}^2 + H_{13}^2 + H_{23}^2)\right\} \end{aligned}$$

$$
\begin{aligned}
&+\frac{1}{18}(H_{13}^2+H_{23}^2)\left[(H_{11}-H_{22})^2+4H_{12}^2\right]+\frac{1}{9}(H_{13}^2+H_{23}^2)^2\\
&+\frac{1}{144}\left[(H_{11}-H_{22})^2+4H_{12}^2\right]^2.
\end{aligned}
$$

Making use of the double degeneracy of the states, we recognize that the secular equation can be rewritten as

$$(x-a)^2=0,$$

where

$$
\begin{aligned}
x&=\left[\frac{1}{6}(4H_{33}+H_{11}+H_{22})-\lambda\right]\left[\frac{1}{2}(H_{11}+H_{22})-\lambda\right],\\
a&=\frac{1}{12}\left[(H_{11}-H_{22})^2+4H_{12}^2+4(H_{13}^2+H_{23}^2)\right].
\end{aligned}
$$

Then, writing $x=a$, we have

$$
\begin{aligned}
&\left[\frac{1}{6}(4H_{33}+H_{11}+H_{22})-\lambda\right]\left[\frac{1}{2}(H_{11}+H_{22})-\lambda\right]\\
&=\frac{1}{12}\left[(H_{11}-H_{22})^2+4H_{12}^2+4(H_{13}^2+H_{23}^2)\right],
\end{aligned}
$$

or

$$
\begin{aligned}
&\lambda^2-\left[\frac{4}{3}(H_{11}+H_{22}+H_{33})\right]\lambda+\frac{1}{12}(4H_{33}+H_{11}+H_{22})(H_{11}+H_{22})\\
&-\frac{1}{12}\left[(H_{11}-H_{22})^2+4(H_{12}^2+H_{13}^2+H_{23}^2)\right]=0.
\end{aligned}
\tag{3.46}
$$

The eigenvalues are

$$
\begin{aligned}
\lambda&=\frac{1}{3}(H_{11}+H_{22}+H_{33})\pm\frac{1}{2}\left\{\frac{4}{9}(H_{11}+H_{22}+H_{33})^2\right.\\
&\quad\left.+\frac{1}{3}\left[(H_{11}-H_{22})^2+4(H_{12}^2+H_{13}^2+H_{23}^2)-(H_{11}+H_{22})(4H_{33}+H_{11}+H_{22})\right]\right\}^{1/2}\\
&=\frac{1}{3}(L+2M)k^2\pm\left\{\frac{1}{9}(L+2M)^2k^4+\frac{N^2}{3}(k_x^2k_y^2+k_y^2k_z^2+k_z^2k_x^2)\right.\\
&\quad\left.+\frac{1}{12}\left[(H_{11}-H_{22})^2-(H_{11}+H_{22})(4H_{33}+H_{11}+H_{22})\right]\right\}^{1/2}.
\end{aligned}
\tag{3.47}
$$

It remains to simplify the last term of Eq. (3.47). Note that

$$\frac{1}{12}\left[(H_{11}-H_{22})^2-(H_{11}+H_{22})(4H_{33}+H_{11}+H_{22})\right]$$

$$
\begin{aligned}
&= \frac{1}{12}\left[(H_{11} - H_{22})^2 - (H_{11} + H_{22})^2 - 4H_{33}(H_{11} + H_{22})\right] \\
&= -\frac{1}{3}\left[H_{11}H_{22} + H_{22}H_{33} + H_{33}H_{11}\right] \\
&= -\frac{1}{3}\left[(L^2 + 3M^2)(k_x^2k_y^2 + k_y^2k_z^2 + k_z^2k_x^2) + M^2(k_x^4 + k_y^4 + k_z^4)\right. \\
&\quad \left. +2ML(k_x^4 + k_y^4 + k_z^4 + k_x^2k_y^2 + k_y^2k_z^2 + k_z^2k_x^2)\right], \qquad (3.48)
\end{aligned}
$$

while

$$
\begin{aligned}
\frac{1}{9}(L + 2M)^2k^4 &= \frac{1}{9}(L - M)^2k^4 + M^2k^4 + \frac{2}{3}M(L - M)k^4 \\
&= \frac{1}{9}(L - M)^2k^4 + \frac{M}{3}(2L + M)k^4. \qquad (3.49)
\end{aligned}
$$

Combining Eq. (3.48) with the second term on the right-hand side of Eq. (3.49) and using

$$
k^4 = (k_x^2 + k_y^2 + k_z^2)^2 = (k_x^4 + k_y^4 + k_z^4) + 2(k_x^2k_y^2 + k_y^2k_z^2 + k_z^2k_x^2),
$$

we finally get

$$
\begin{aligned}
&\frac{1}{3}\Big\{M(2L + M)k^4 - [(L^2 + 3M^2)(k_{xy} + k_{yz} + k_{zx}) + M^2(k_x^4 + k_y^4 + k_z^4) \\
&+2ML(k_x^4 + k_y^4 + k_z^4 + k_{xy} + k_{yz} + k_{zx})]\Big\} = \frac{1}{3}(L - M)^2(k_{xy} + k_{yz} + k_{zx}),
\end{aligned}
$$

where we have written

$$
k_{xy} + k_{yz} + k_{zx} \equiv k_x^2k_y^2 + k_y^2k_z^2 + k_z^2k_x^2.
$$

Hence, the dispersion is

$$
\begin{aligned}
E(\mathbf{k}) &= \frac{1}{3}(L + 2M)k^2 \pm \left\{\frac{1}{9}(L - M)^2k^4 + \frac{1}{3}\left[N^2 - (L - M)^2\right](k_x^2k_y^2 + k_y^2k_z^2 + k_z^2k_x^2)\right\}^{1/2} \\
&\equiv Ak^2 \pm \left[B^2k^4 + C^2(k_x^2k_y^2 + k_y^2k_z^2 + k_z^2k_x^2)\right]^{1/2}, \qquad (3.50)
\end{aligned}
$$

where

$$
\begin{aligned}
A &= \frac{1}{3}(L + 2M) + \frac{\hbar^2}{2m_0}, \\
B &= \frac{1}{3}(L - M), \qquad (3.51)
\end{aligned}
$$

$$C^2 = \frac{1}{3}\left[N^2 - (L-M)^2\right].$$

Note that these solutions are identical to Eqs. (3.13) and (3.14).

3.3.3 Kane Solution

Kane [3] sought to block diagonalize the Hamiltonian as much as possible via unitary transformations before looking for analytic solutions. The key is to recognize the structure of the Hamiltonian matrix, here due to time-reversal symmetry. The Kramers operator for a crystal with inversion is

$$\mathcal{K} = -\mathrm{i}\sigma_y \mathcal{C} I, \tag{3.52}$$

where I is the inversion operator and $\mathcal{C}$ is complex conjugation. The basis can then be written as

$$\phi_1, \phi_2, \phi_3, \mathcal{K}\phi_1, \mathcal{K}\phi_2, \mathcal{K}\phi_3. \tag{3.53}$$

Here, they correspond to

$$\left|\frac{3}{2}\,\frac{3}{2}\right\rangle, \left|\frac{3}{2}\,\frac{1}{2}\right\rangle, \left|\frac{1}{2}\,\frac{1}{2}\right\rangle, \left|\frac{3}{2}\,-\frac{3}{2}\right\rangle, \left|\frac{3}{2}\,-\frac{1}{2}\right\rangle, \left|\frac{1}{2}\,-\frac{1}{2}\right\rangle.$$

Since $\mathcal{K}$ is equivalent to the time-reversed symmetry operator, the states ϕ_i and $\mathcal{K}\phi_i$ differ in their m values: $\pm m$, respectively. Luttinger and Kohn [6], on the other hand, defined the time-reversal operator as

$$\mathcal{K} = \sigma_y \mathcal{C}. \tag{3.54}$$

The $|J\,+|m|\rangle$ states of LK differ from ours; since $\mathcal{K}$ is also different, the $|J\,-|m|\rangle$ states differ as well. We have,

$$\begin{aligned}
\langle \mathcal{K}\phi_i|\mathcal{K}\phi_j\rangle &= \langle \phi_i|\phi_j\rangle^*,\\
\langle \mathcal{K}\phi_i|H|\mathcal{K}\phi_j\rangle &= \langle \phi_i|H|\phi_j\rangle^*,\\
\langle \phi_i|H|\mathcal{K}\phi_j\rangle &= -\langle \phi_j|H|\mathcal{K}\phi_i\rangle.
\end{aligned} \tag{3.55}$$

We, therefore, reorder the transformation matrix S from Eq. (3.39) into U defined by

$$U = \left(\begin{array}{ccccccc} & \left|\frac{3}{2}\ \frac{3}{2}\right\rangle & \left|\frac{3}{2}\ \frac{1}{2}\right\rangle & \left|\frac{1}{2}\ \frac{1}{2}\right\rangle & \left|\frac{3}{2}\ -\frac{3}{2}\right\rangle & \left|\frac{3}{2}\ -\frac{1}{2}\right\rangle & \left|\frac{1}{2}\ -\frac{1}{2}\right\rangle \\ |\varepsilon_1^+\uparrow\rangle & \frac{1}{\sqrt{2}} & 0 & 0 & 0 & -\frac{1}{\sqrt{6}} & -\frac{1}{\sqrt{3}} \\ |\varepsilon_2^+\uparrow\rangle & \frac{\mathrm{i}}{\sqrt{2}} & 0 & 0 & 0 & \frac{\mathrm{i}}{\sqrt{6}} & \frac{\mathrm{i}}{\sqrt{3}} \\ |\varepsilon_3^+\uparrow\rangle & 0 & -\sqrt{\frac{2}{3}} & \frac{1}{\sqrt{3}} & 0 & 0 & 0 \\ |\varepsilon_1^+\downarrow\rangle & 0 & \frac{1}{\sqrt{6}} & \frac{1}{\sqrt{3}} & \frac{1}{\sqrt{2}} & 0 & 0 \\ |\varepsilon_2^+\downarrow\rangle & 0 & \frac{\mathrm{i}}{\sqrt{6}} & \frac{\mathrm{i}}{\sqrt{3}} & -\frac{\mathrm{i}}{\sqrt{2}} & 0 & 0 \\ |\varepsilon_3^+\downarrow\rangle & 0 & 0 & 0 & 0 & -\sqrt{\frac{2}{3}} & \frac{1}{\sqrt{3}} \end{array}\right). \tag{3.56}$$

Our U differs from Kane's Eq. (10) [3] by an overall sign but otherwise has the same ordering. Thus, the Hamiltonian can be written as (using Kane's basis ordering)

$$H = \begin{pmatrix} G & \Gamma \\ -\Gamma^* & G^* \end{pmatrix}, \tag{3.57}$$

where $\Gamma^T = -\Gamma$. Note that our U in Eq. (3.56) is of this form too:

$$U = \begin{pmatrix} S & R \\ -R^* & S^* \end{pmatrix}.$$

Comparing Eq. (3.57) with Table 3.5 and accounting for the ordering difference, we find

$$G = \begin{pmatrix} \frac{H_{11}+H_{22}}{2} & \frac{-H_{13}+\mathrm{i}H_{23}}{\sqrt{3}} & \frac{H_{13}-\mathrm{i}H_{23}}{\sqrt{6}} \\ \frac{-H_{13}-\mathrm{i}H_{23}}{\sqrt{3}} & \frac{H_{11}+H_{22}+4H_{33}}{6} & \frac{H_{11}+H_{22}-2H_{33}}{3\sqrt{2}} \\ \frac{H_{13}+\mathrm{i}H_{23}}{\sqrt{6}} & \frac{H_{11}+H_{22}-2H_{33}}{3\sqrt{2}} & \frac{H_{11}+H_{22}+H_{33}}{3} - \Delta_0 \end{pmatrix}, \tag{3.58}$$

$$\Gamma = \begin{pmatrix} 0 & \frac{-H_{11}+H_{22}+2\mathrm{i}H_{12}}{2\sqrt{3}} & \frac{-H_{11}+H_{22}+2\mathrm{i}H_{12}}{\sqrt{6}} \\ \frac{H_{11}-H_{22}-2\mathrm{i}H_{12}}{2\sqrt{3}} & 0 & \frac{H_{13}-\mathrm{i}H_{23}}{\sqrt{2}} \\ \frac{H_{11}-H_{22}-2\mathrm{i}H_{12}}{\sqrt{6}} & \frac{-H_{13}+\mathrm{i}H_{23}}{\sqrt{2}} & 0 \end{pmatrix}. \tag{3.59}$$

Following Kane, we introduce

$$\begin{aligned} X\mathrm{e}^{\mathrm{i}\chi} &= -H_{11} + H_{22} + 2\mathrm{i}H_{12}, \\ Y\mathrm{e}^{\mathrm{i}\eta} &= H_{13} - \mathrm{i}H_{23}, \\ Z &= H_{11} + H_{22} - 2H_{33}. \end{aligned} \tag{3.60}$$

One can then show that the following transformation

$$U_1 = \begin{pmatrix} S_1 & R_1 \\ -R_1^* & S_1^* \end{pmatrix},$$

with

$$S_1 = \frac{1}{\sqrt{2}} \begin{pmatrix} e^{i\left(\frac{\chi+\eta}{2}-\frac{\pi}{4}\right)} & 0 & 0 \\ 0 & e^{i\left(\frac{\chi-\eta}{2}-\frac{\pi}{4}\right)} & 0 \\ 0 & 0 & e^{i\left(\frac{\chi-\eta}{2}-\frac{\pi}{4}\right)} \end{pmatrix}, \tag{3.61}$$

$$R_1 = \frac{1}{\sqrt{2}} \begin{pmatrix} -e^{i\left(\frac{\chi+\eta}{2}-\frac{\pi}{4}\right)} & 0 & 0 \\ 0 & -e^{i\left(\frac{\chi-\eta}{2}-\frac{\pi}{4}\right)} & 0 \\ 0 & 0 & -e^{i\left(\frac{\chi-\eta}{2}-\frac{\pi}{4}\right)} \end{pmatrix}, \tag{3.62}$$

transforms the Hamiltonian into

$$H' = \begin{pmatrix} G' & \Gamma' \\ -\Gamma'^* & G'^* \end{pmatrix}, \tag{3.63}$$

where

$$G' = \begin{pmatrix} \frac{H_{11}+H_{22}}{2} & \frac{-Y+iX/2}{\sqrt{3}} & \frac{Y+iX}{\sqrt{6}} \\ \frac{Y-iX/2}{\sqrt{3}} & \frac{H_{11}+H_{22}+4H_{33}}{6} & \frac{Z/3+iY\cos(\chi-2\eta)}{\sqrt{2}} \\ \frac{Y-iX}{\sqrt{6}} & \frac{Z/3-iY\cos(\chi-2\eta)}{\sqrt{2}} & \frac{H_{11}+H_{22}+H_{33}}{3}-\Delta_0 \end{pmatrix}, \tag{3.64}$$

$$\Gamma' = \begin{pmatrix} 0 & 0 & 0 \\ 0 & 0 & \frac{Y\sin(\chi-2\eta)}{\sqrt{2}} \\ 0 & \frac{-Y\sin(\chi-2\eta)}{\sqrt{2}} & 0 \end{pmatrix}. \tag{3.65}$$

Obviously, Γ' is zero for certain values of the wave vector; in that case, the Hamiltonian is block diagonal.

3.4 Wurtzite

Another important type of band structure is that of wurtzite-type materials.

3.4.1 Overview

The band structure and optical properties were first studied in the late 1950s [37–40]. Pikus [41] obtained the valence band using the method of invariants and provided a six-band model. Gutsche and Jahne [42] wrote down a 12-band model for the valence band at $\mathbf{k} = \mathbf{0}$. The bulk band structure regained attention in the 1990s due to the growth of high-quality epitaxial GaN and AlN. Thus, Sirenko and coworkers extended the study of the valence band [43–45] while Chuang and coworkers

[46, 47] introduced a Kane model and also used perturbation theory to compare to the invariant method. A coupled conduction-valence band model was introduced by Lew Yan Voon et al. [48], in which the conduction state was folded into the valence block and the latter diagonalized exactly. A treatment where they are treated on an equal footing was by Andreev and O'Reilly in 2000 [49] and used subsequently [50, 51]. Band parameters for a number of wurtzite (WZ) materials have now been obtained [45, 46, 52, 53]. There have also been a number of studies for nanostructures [43, 46, 47, 54–58].

Some basic differences compared to the ZB problem are:

- The symmetry is hexagonal [C_{6v}^4 (6 mm)] instead of cubic.
- The six-band valence Hamiltonian now has 10 parameters (seven A_i and three Δ_i) instead of four.
- The bulk Hamiltonian with spin-orbit interaction cannot be diagonalized exactly at $\mathbf{k} = \mathbf{0}$ using only symmetry-adapted functions.

The WZ semiconductors are generally large-band-gap materials (except for InN with a band gap of ~ 0.7 eV [59, 60]) with a direct gap at the Γ point. The presence of both a crystal-field splitting (compared to a cubic structure) and spin-orbit interaction leads to a complex valence-band structure consisting of three doubly-degenerate bands at the Γ point; they are known as the A, B, and C bands.

Just as for the cubic semiconductors, the band structure near the Γ point will be of interest. One complication is that basis states that transforms as $s, p, d, ...$ will no longer diagonalize the Hamiltonian even at that point. This is clear from the irreducible basis functions given in Table B.10.

3.4.2 Basis States

Different models for the band structure of WZ materials have been considered, corresponding to different basis functions. In Table C.9, we list together the main choices of basis states. We have maintained the notation in the original papers, whereby the basis functions for, e.g., Chuang and Chang [46] are given in capital letters whereas the ones for Gutsche and Jahne [42] are in small letters. As noted by Chuang and Chang [46], other work have been less explicit in their basis functions and, as a result, discrepancies have arisen among the various Hamiltonians to be found in the literature. For example, Pikus [1, 61] and Sirenko et al. [43] only mention that they used the LS and JM_J basis without giving the full representations. As we did for ZB materials, we will provide as complete a picture as we can regarding the various Hamiltonians and the corresponding basis functions.

3.4.3 Chuang–Chang Hamiltonian

The presentation of the Hamiltonian within perturbation theory was done by Chuang and Chang (CC) [46].

Both spin-orbit and crystal-field splitting are important for WZ materials; hence, it is common to use basis functions that reflect this. The Hamiltonian consists of two terms–one with constant energies, and one k-dependent:

$$H(\mathbf{k}) = H_{k=0} + D_{6\times 6}(\mathbf{k}), \tag{3.66}$$

where the D matrix was defined in Eq. (3.6). As WZ differs from ZB by the inequivalence of the z axis from x and y, one can use a basis that resembles the JM_J states for cubic crystals but with the Z function separate. This is the so-called u basis and is given in Table 3.7.

Table 3.7 *u* basis states for the valence bands of wurtzite [46]

				J_z
Γ_5	$\|u_1\rangle$	$-\frac{1}{\sqrt{2}}\|(X+\mathrm{i}Y)\uparrow\rangle$	$Y_{1\ 1}\uparrow$	$\frac{3}{2}$
Γ_5	$\|u_2\rangle$	$\frac{1}{\sqrt{2}}\|(X-\mathrm{i}Y)\uparrow\rangle$	$Y_{1\,-1}\uparrow$	$-\frac{1}{2}$
Γ_1	$\|u_3\rangle$	$\|Z\uparrow\rangle$	$Y_{1\ 0}\uparrow$	$\frac{1}{2}$
Γ_5	$\|u_4\rangle$	$\frac{1}{\sqrt{2}}\|(X-\mathrm{i}Y)\downarrow\rangle$	$Y_{1\,-1}\downarrow$	$-\frac{3}{2}$
Γ_5	$\|u_5\rangle$	$-\frac{1}{\sqrt{2}}\|(X+\mathrm{i}Y)\downarrow\rangle$	$Y_{1\ 1}\downarrow$	$\frac{1}{2}$
Γ_1	$\|u_6\rangle$	$\|Z\downarrow\rangle$	$Y_{1\ 0}\downarrow$	$-\frac{1}{2}$

3.4.3.1 $H_{k=0}$

We have [using Eq. (3.32)],

$$H_{k=0} = H_0 + H_{\mathrm{so}} = H_0 + H_{\mathrm{s},i}\sigma_i. \tag{3.67}$$

In the u basis, for example,

$$\begin{aligned}
&\langle u_1|H_{k=0}|u_1\rangle = \langle -\frac{1}{\sqrt{2}}(X+\mathrm{i}Y)\uparrow|H|-\frac{1}{\sqrt{2}}(X+\mathrm{i}Y)\uparrow\rangle\\
&= \frac{1}{2}\left[\langle X\uparrow|H_0|X\uparrow\rangle + \langle Y\uparrow|H_0|Y\uparrow\rangle + \mathrm{i}\langle X|H_{\mathrm{s},z}|Y\rangle\langle\uparrow|\sigma_z|\uparrow\rangle - \mathrm{i}\langle Y|H_{\mathrm{s},z}|X\rangle\langle\uparrow|\sigma_z|\uparrow\rangle\right]\\
&= \langle X|H_0|X\rangle + \frac{\mathrm{i}}{2}\left[\langle X|H_{\mathrm{s},z}|X\rangle - \langle Y|H_{\mathrm{s},z}|X\rangle\right]\\
&\equiv E_v + \Delta_1 + \Delta_2,
\end{aligned}$$

$$\begin{aligned}
\langle u_2|H_{k=0}|u_6\rangle &= \left\langle \frac{1}{\sqrt{2}}(X-\mathrm{i}Y)\uparrow|H_{k=0}|Z\downarrow\right\rangle = \left\langle \frac{1}{\sqrt{2}}(X-\mathrm{i}Y)\uparrow|H_{\mathrm{so}}|Z\downarrow\right\rangle\\
&= \frac{1}{\sqrt{2}}\left[\langle X|H_{\mathrm{s},y}|Z\rangle\langle\uparrow|\sigma_y|\downarrow\rangle + \mathrm{i}\langle Y|H_{\mathrm{s},x}|Z\rangle\langle\uparrow|\sigma_x|\downarrow\rangle\right]\\
&= \frac{1}{\sqrt{2}}\left[-\mathrm{i}\langle X|H_{\mathrm{s},y}|Z\rangle + \mathrm{i}\langle Y|H_{\mathrm{s},x}|Z\rangle\right]\\
&\equiv \sqrt{2}\Delta_3.
\end{aligned}$$

Then $H_{k=0}$ in the u representation is

$$H_{k=0} = \left(\begin{array}{cccccc} |u_1\rangle & |u_2\rangle & |u_3\rangle & |u_4\rangle & |u_5\rangle & |u_6\rangle \\ E_\nu + \varDelta_1 + \varDelta_2 & 0 & 0 & 0 & 0 & 0 \\ 0 & E_\nu + \varDelta_1 - \varDelta_2 & 0 & 0 & 0 & \sqrt{2}\varDelta_3 \\ 0 & 0 & E_\nu & 0 & \sqrt{2}\varDelta_3 & 0 \\ 0 & 0 & 0 & E_\nu + \varDelta_1 + \varDelta_2 & 0 & 0 \\ 0 & 0 & \sqrt{2}\varDelta_3 & 0 & E_\nu + \varDelta_1 - \varDelta_2 & 0 \\ 0 & \sqrt{2}\varDelta_3 & 0 & 0 & 0 & E_\nu \end{array}\right), \tag{3.68}$$

where

$$\begin{aligned} \langle X|H_0|X\rangle &= \langle Y|H_0|Y\rangle = E_\nu + \varDelta_1, \\ \langle Z|H_0|Z\rangle &= E_\nu, \\ \langle X|H_{s,z}|Y\rangle &= -\mathrm{i}\varDelta_2, \\ \langle Y|H_{s,x}|Z\rangle &= \langle Z|H_{s,y}|X\rangle = -\mathrm{i}\varDelta_3, \end{aligned} \tag{3.69}$$

3.4.3.2 $D_{6\times6}(\mathbf{k})$

Since $D_{6\times6}(\mathbf{k})$ does not include the spin-orbit interaction, its matrix representation in the LS basis can be written as

$$D_{6\times6} = \left(\begin{array}{cc} \uparrow & \downarrow \\ D_{3\times3} & 0 \\ 0 & D_{3\times3} \end{array}\right). \tag{3.70}$$

For $D_{3\times3}$, one can start with the Hamiltonian in the X, Y, Z basis:

$$D_{3\times3} = \left(\begin{array}{ccc} |X\rangle & |Y\rangle & |Z\rangle \\ L_1k_x^2 + M_1k_y^2 + M_2k_z^2 & N_1k_xk_y & N_2k_xk_z \\ N_1k_xk_y & M_1k_x^2 + L_1k_y^2 + M_2k_z^2 & N_2k_yk_z \\ N_2k_zk_x & N_2k_zk_y & M_1(k_x^2 + k_y^2) + L_2k_z^2 \end{array}\right). \tag{3.71}$$

We have

$$\begin{aligned} L_1 &= \frac{\hbar^2}{2m_0}\left(1 + \sum_l^B \frac{2p_{Xl}^x p_{lX}^x}{m_0(E_0 - E_l)}\right) = \frac{\hbar^2}{2m_0}\left(1 + \sum_l^B \frac{2p_{Yl}^y p_{lY}^y}{m_0(E_0 - E_l)}\right), \\ L_2 &= \frac{\hbar^2}{2m_0}\left(1 + \sum_l^B \frac{2p_{Zl}^z p_{lZ}^z}{m_0(E_0 - E_l)}\right), \end{aligned}$$

$$
\begin{aligned}
M_1 &= \frac{\hbar^2}{2m_0}\left(1+\sum_l^B \frac{2p_{Xl}^y p_{lX}^y}{m_0(E_0-E_l)}\right) = \frac{\hbar^2}{2m_0}\left(1+\sum_l^B \frac{2p_{Yl}^x p_{lY}^x}{m_0(E_0-E_l)}\right),\\
M_2 &= \frac{\hbar^2}{2m_0}\left(1+\sum_l^B \frac{2p_{Xl}^z p_{lX}^z}{m_0(E_0-E_l)}\right) = \frac{\hbar^2}{2m_0}\left(1+\sum_l^B \frac{2p_{Yl}^z p_{lY}^z}{m_0(E_0-E_l)}\right),\\
M_3 &= \frac{\hbar^2}{2m_0}\left(1+\sum_l^B \frac{2p_{Zl}^x p_{lZ}^x}{m_0(E_0-E_l)}\right) = \frac{\hbar^2}{2m_0}\left(1+\sum_l^B \frac{2p_{Zl}^y p_{lZ}^y}{m_0(E_0-E_l)}\right),\\
N_1 &= \frac{\hbar^2}{m_0^2}\sum_l^B \frac{p_{Xl}^x p_{lY}^y + p_{Xl}^y p_{lY}^x}{(E_0-E_l)},\\
N_2 &= \frac{\hbar^2}{m_0}\left(1+\sum_l^B \frac{p_{Xl}^x p_{lZ}^z + p_{Xl}^z p_{lZ}^x}{m_0(E_0-E_l)}\right) = \frac{\hbar^2}{m_0}\left(1+\sum_l^B \frac{p_{Yl}^y p_{lZ}^z + p_{Yl}^z p_{lZ}^y}{m_0(E_0-E_l)}\right),
\end{aligned}
\tag{3.72}
$$

where $p_{Xl}^y = \langle X|p_y|l\rangle$, …The matrix can now be written in the u basis. For example,

$$
\begin{aligned}
\langle u_1|D|u_1\rangle &= \frac{1}{2}\langle (X+\mathrm{i}Y)\uparrow|D|(X+\mathrm{i}Y)\uparrow\rangle\\
&= \frac{1}{2}\left[\langle X|D|X\rangle + \langle Y|D|Y\rangle + \mathrm{i}\left(\langle X|D|Y\rangle - \langle Y|D|X\rangle\right)\right]\\
&= \frac{1}{2}(L_1+M_1)(k_x^2+k_y^2) + M_2k_z^2 \equiv D_{11},\\
\langle u_3|D|u_3\rangle &= \langle Z\uparrow|D|Z\uparrow\rangle = M_3(k_x^2+k_y^2) + M_2k_z^2 \equiv D_{33},\\
\langle u_2|D|u_1\rangle &= \frac{1}{2}\langle (X-\mathrm{i}Y)\uparrow|D|(X+\mathrm{i}Y)\uparrow\rangle\\
&= \frac{1}{2}(L_1-M_1)(k_x^2-k_y^2) + \mathrm{i}N_1k_xk_y \equiv D_{21},\\
\langle u_2|D|u_3\rangle &= \frac{1}{\sqrt{2}}\langle (X-\mathrm{i}Y)\uparrow|D|Z\uparrow\rangle = \frac{1}{\sqrt{2}}N_2k_z(k_x+\mathrm{i}k_y).
\end{aligned}
$$

The D matrix is then

$$
\begin{pmatrix}
D_{11} & D_{21}^* & -D_{23}^* & & & \\
D_{21} & D_{11} & D_{23} & & 0 & \\
-D_{23} & D_{23}^* & D_{33} & & & \\
 & & & D_{11} & D_{21} & D_{23}\\
 & & & D_{21}^* & D_{11} & -D_{23}^*\\
 & & & D_{23}^* & -D_{23} & D_{33}
\end{pmatrix}.
\tag{3.73}
$$

The complete Hamiltonian matrix is given in Table 3.8. For WZ, we have [46]

$$L_1 - M_1 = N_1. \tag{3.74}$$

Table 3.8 Six-band Chuang–Chang Hamiltonian in u basis

$$H_{CC}(\mathbf{k}) = \left(\begin{array}{cccccc} |u_1\rangle & |u_2\rangle & |u_3\rangle & |u_4\rangle & |u_5\rangle & |u_6\rangle \\ F & -K^* & -H^* & 0 & 0 & 0 \\ -K & G & H & 0 & 0 & \Delta \\ -H & H^* & \lambda & 0 & \Delta & 0 \\ 0 & 0 & 0 & F & -K & H \\ 0 & 0 & \Delta & -K^* & G & -H^* \\ 0 & \Delta & 0 & H^* & -H & \lambda \end{array}\right),$$

where

$$\begin{aligned} F &= \Delta_1 + \Delta_2 + \lambda + \theta, \\ G &= \Delta_1 - \Delta_2 + \lambda + \theta, \\ \lambda &= L_2 k_z^2 + M_3(k_x^2 + k_y^2), \\ \theta &= (M_2 - L_2)k_z^2 + (\frac{L_1 + M_1}{2} - M_3)(k_x^2 + k_y^2), \\ K &= \frac{N_1}{2}(k_x + \mathrm{i}k_y)^2, \\ H &= \frac{N_2}{\sqrt{2}}(k_x + \mathrm{i}k_y)k_z, \\ \Delta &= \sqrt{2}\Delta_3. \end{aligned}$$

The model has an exact solution at $\mathbf{k} = \mathbf{0}$. The following states are decoupled: $|u_1\rangle$, and $|u_4\rangle$. There are two coupled pairs: $|u_2\rangle$ and $|u_6\rangle$, and $|u_3\rangle$ and $|u_5\rangle$. The energies are $E_1 = E_v + \Delta_1 + \Delta_2$, and

$$E_2 = E_v + \frac{(\Delta_1 - \Delta_2)}{2} + \sqrt{\left(\frac{(\Delta_1 - \Delta_2)}{2}\right)^2 + 2\Delta_3^2}, \tag{3.75}$$

$$E_3 = E_v + \frac{(\Delta_1 - \Delta_2)}{2} - \sqrt{\left(\frac{(\Delta_1 - \Delta_2)}{2}\right)^2 + 2\Delta_3^2}. \tag{3.76}$$

An example band structure for GaN is shown in Fig. 3.4. The band structure was obtained from an ab initio calculation and fitted to the RSP Hamiltonian. The latter is equivalent to the CC Hamiltonian and will be introduced in Chap. **??**. The bands are plotted along $\Gamma - A$ ($k_{||}$) and along two directions perpendicular to $k_{||}$. In-plane anisotropy is observed by the difference between the two $k_\perp$ directions.

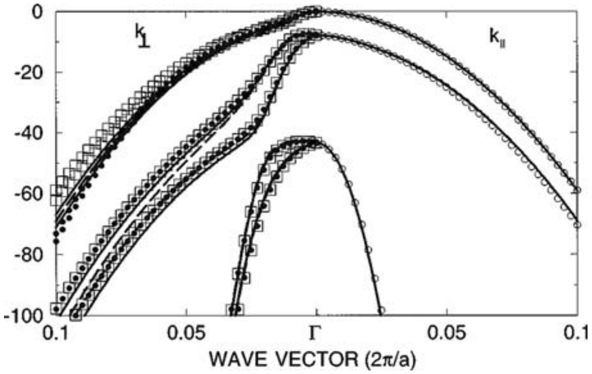

Fig. 3.4 GaN valence-band structure from an ab initio calculation with a fit to the RSP Hamiltonian(solid line). $k_{||}$ corresponds to $\Gamma - A$. *Open squares*: $\Gamma - K$ direction; *filled circles*: $\Gamma - M$ direction. *Dashed curve* is a fit without the A_7 term. Reprinted with permission from [62]. ©1997 by the American Physical Society

3.4.3.3 Block Diagonalization

A block diagonalization scheme can be written down. This was first carried out by Sirenko et al.[43] and Chuang and Chang [46]. The trick is to recognize that the vectors have azimuthal symmetry in the x-y plane. The choice

$$k_x + \mathrm{i}k_y = k_{||}\mathrm{e}^{\mathrm{i}\phi} \tag{3.77}$$

leads to the off-diagonal matrix elements being written as

$$K = K_{||}\mathrm{e}^{2\mathrm{i}\phi},\ K_{||} = \frac{N_1}{2}k_{||}^2, \tag{3.78}$$

$$H = H_{||}\mathrm{e}^{\mathrm{i}\phi},\ H_{||} = \frac{N_2}{\sqrt{2}}k_{||}k_z. \tag{3.79}$$

The explicit ϕ dependence can then be eliminated by rescaling the basis functions [15]:

$$u_1' = \mathrm{e}^{-\frac{3\mathrm{i}}{2}\phi}u_1,$$

$$u_2' = \mathrm{e}^{\frac{\mathrm{i}}{2}\phi}u_2,$$

$$u_3' = \mathrm{e}^{-\frac{\mathrm{i}}{2}\phi}u_3,$$

$$u'_4 = \mathrm{e}^{\frac{3\mathrm{i}}{2}\phi} u_4, \tag{3.80}$$

$$u'_5 = \mathrm{e}^{-\frac{\mathrm{i}}{2}\phi} u_5,$$

$$u'_6 = \mathrm{e}^{\frac{\mathrm{i}}{2}\phi} u_6,$$

or $|u'_i\rangle = \sum_j T_{ij} |u_j\rangle$, where

$$T = \begin{pmatrix} \alpha^* & 0 & 0 & \alpha & 0 & 0 \\ 0 & \beta & 0 & 0 & \beta^* & 0 \\ 0 & 0 & \beta^* & 0 & 0 & \beta \\ \alpha^* & 0 & 0 & -\alpha & 0 & 0 \\ 0 & \beta & 0 & 0 & -\beta^* & 0 \\ 0 & 0 & -\beta^* & 0 & 0 & \beta \end{pmatrix}, \tag{3.81}$$

and

$$\alpha = \frac{1}{\sqrt{2}} \mathrm{e}^{\mathrm{i}(\frac{3}{4}\pi + \frac{3}{2}\phi)}, \ \beta = \frac{1}{\sqrt{2}} \mathrm{e}^{\mathrm{i}(\frac{1}{4}\pi + \frac{1}{2}\phi)}. \tag{3.82}$$

Finally, the Hamiltonian matrix becomes

$$H'(\mathbf{k}) = \begin{pmatrix} F & K_{||} & -\mathrm{i}H_{||} & 0 & 0 & 0 \\ K_{||} & G & \Delta - \mathrm{i}H_{||} & 0 & 0 & 0 \\ \mathrm{i}H_{||} & \Delta + \mathrm{i}H_{||} & \lambda & 0 & 0 & 0 \\ 0 & 0 & 0 & F & K_{||} & \mathrm{i}H_{||} \\ 0 & 0 & 0 & K_{||} & G & \Delta + \mathrm{i}H_{||} \\ 0 & 0 & 0 & -\mathrm{i}H_{||} & \Delta - \mathrm{i}H_{||} & \lambda \end{pmatrix}. \tag{3.83}$$

3.4.4 Gutsche–Jahne Hamiltonian

The basis for the above CC model consisted of the three Y^1_m functions together with the two-component spin function. The spatial functions only transformed according to Γ_1 and Γ_5. In the Gutsche–Jahne (GJ) basis, spatial functions transforming according to Γ_1, Γ_5, Γ_3 and Γ_6 are used (Table 3.9).

Hence, the GJ model is a 12-band model with spin for the valence band of WZ. Note, however, that they only set up the Hamiltonian at the Γ point. In the GJ basis, $H_{k=0}$ actually block diagonalizes into two 6×6 blocks as the last six states are Kramers partners of the top six:

$$H(\mathbf{k}) = \begin{pmatrix} S & 0 \\ 0 & S^* \end{pmatrix}. \tag{3.84}$$

where

Table 3.9 Basis set for wurtzite: Gutsche–Jahne [42]

Γ_5	$\lvert u_5^* \uparrow\rangle$	$\lvert (x - \mathrm{i}y) \uparrow\rangle$
Γ_1	$\lvert u_1 \downarrow\rangle$	$\lvert z \downarrow\rangle$
Γ_6	$\lvert u_6 \uparrow\rangle$	$\lvert (x + \mathrm{i}y)^2 \uparrow\rangle$
Γ_3	$\lvert u_3 \downarrow\rangle$	$\lvert x(3y^2 - x^2) \downarrow\rangle$
Γ_5	$\lvert u_5 \uparrow\rangle$	$\lvert (x + \mathrm{i}y) \uparrow\rangle$
Γ_6	$\lvert u_6 \downarrow\rangle$	$\lvert (x + \mathrm{i}y)^2 \downarrow\rangle$
Γ_5	$\lvert u_5 \downarrow\rangle$	$\lvert (x + \mathrm{i}y) \downarrow\rangle$
Γ_1	$\lvert - u_1 \uparrow\rangle$	$\lvert - z \uparrow\rangle$
Γ_6	$\lvert u_6^* \downarrow\rangle$	$\lvert (x - \mathrm{i}y)^2 \downarrow\rangle$
Γ_3	$\lvert - u_3 \uparrow\rangle$	$\lvert x(x^2 - 3y^2) \uparrow\rangle$
Γ_5	$\lvert u_5^* \downarrow\rangle$	$\lvert (x - \mathrm{i}y) \downarrow\rangle$
Γ_6	$\lvert - u_6^* \uparrow\rangle$	$\lvert - (x - \mathrm{i}y)^2 \uparrow\rangle$

$$S = \left(\begin{array}{cccccc} \lvert u_5^* \uparrow\rangle & \lvert u_1 \downarrow\rangle & \lvert u_6 \uparrow\rangle & \lvert u_3 \downarrow\rangle & \lvert u_5 \uparrow\rangle & \lvert u_6 \downarrow\rangle \\ E_5 - \frac{\Delta_5}{3} & \frac{\sqrt{2}}{3}\Delta_7^* & 0 & 0 & 0 & 0 \\ \frac{\sqrt{2}}{3}\Delta_7 & E_1 & 0 & 0 & 0 & 0 \\ & & E_6 + \frac{\Delta_6}{3} & \frac{\Delta_8^*}{3} & 0 & 0 \\ & & \frac{\Delta_8}{3} & E_3 & 0 & 0 \\ & & & & E_5 + \frac{\Delta_5}{3} & \frac{\sqrt{2}}{3}\Delta_9^* \\ & & & & \frac{\sqrt{2}}{3}\Delta_9 & E_6 - \frac{\Delta_6}{3} \end{array} \right), \tag{3.85}$$

$$\begin{aligned} \frac{\Delta_5}{3} &= \langle u_5 | H_{\mathrm{s},z} | u_5 \rangle, & \frac{\Delta_6}{3} &= \langle u_6 | H_{\mathrm{s},z} | u_6 \rangle, \\ \frac{\Delta_7}{3} &= \frac{1}{\sqrt{2}} \langle u_1 | H_{\mathrm{s},+} | u_5^* \rangle, & \frac{\Delta_8}{3} &= \frac{1}{\sqrt{2}} \langle u_3 | H_{\mathrm{s},+} | u_6 \rangle, \\ \frac{\Delta_9}{3} &= \frac{1}{\sqrt{2}} \langle u_6 | H_{\mathrm{s},+} | u_5 \rangle, \end{aligned} \tag{3.86}$$

with $H_{\mathrm{s},+} = H_{\mathrm{s},x} + \mathrm{i} H_{\mathrm{s},y}$.

The GJ Hamiltonian can be diagonalized exactly. The energies are [42]:

$$\begin{aligned} E_7 &= \frac{1}{2} \left\{ (E_5 + E_1) - \frac{\Delta_5}{3} \pm \sqrt{\left[(E_5 - E_1) - \frac{\Delta_5}{3} \right]^2 + \frac{8}{9} |\Delta_7|^2} \right\}, \\ E_8 &= \frac{1}{2} \left\{ (E_6 + E_3) - \frac{\Delta_6}{3} \pm \sqrt{\left[(E_6 - E_3) - \frac{\Delta_6}{3} \right]^2 + \frac{8}{9} |\Delta_8|^2} \right\}, \\ E_9 &= \frac{1}{2} \left\{ (E_6 + E_5) - \frac{\Delta_5 - \Delta_6}{3} \pm \sqrt{\left[(E_5 - E_6) - \frac{\Delta_5 + \Delta_6}{3} \right]^2 + \frac{8}{9} |\Delta_9|^2} \right\}, \end{aligned} \tag{3.87}$$

where each of the above energies are doubly-degenerate due to time-reversal symmetry and the corresponding linear combination of basis states is given by

$$\sqrt{1-q^2}|u'\uparrow\rangle + q|u''\downarrow\rangle, \tag{3.88}$$

with

$$\begin{aligned}
\left.\begin{matrix} q_7^2 \\ (1-q_7^2) \end{matrix}\right\} &= \frac{1}{2}\left[1 \mp \frac{E_5 - E_1 - \frac{\Delta_5}{3}}{\sqrt{\left[E_5 - E_1 - \frac{\Delta_5}{3}\right]^2 + \frac{8}{9}|\Delta_7|^2}}\right], \\
\left.\begin{matrix} q_8^2 \\ (1-q_8^2) \end{matrix}\right\} &= \frac{1}{2}\left[1 \mp \frac{E_6 - E_3 + \frac{\Delta_6}{3}}{\sqrt{\left[E_6 - E_3 + \frac{\Delta_6}{3}\right]^2 + \frac{8}{9}|\Delta_8|^2}}\right], \\
\left.\begin{matrix} q_9^2 \\ (1-q_9^2) \end{matrix}\right\} &= \frac{1}{2}\left[1 \mp \frac{E_5 - E_6 + \frac{\Delta_5+\Delta_6}{3}}{\sqrt{\left[E_5 - E_6 + \frac{\Delta_5+\Delta_6}{3}\right]^2 + \frac{8}{9}|\Delta_9|^2}}\right].
\end{aligned} \tag{3.89}$$

As discussed by Gutsche and Jahne [42], this model requires eight parameters (with a ninth set equal to zero) in order to describe the valence-band structure of WZ at $\mathbf{k} = \mathbf{0}$. This is to be contrasted to the $k \cdot p$ theory for ZB, with only one parameter (Δ_0). The structure of WZ can be viewed as starting from the ZB one and straining it along the [111] direction. The consequence in reciprocal space would be a zone folding of ZB bands along the L direction. This is consistent with the doubling of the number of valence bands for WZ compared to ZB. This effect leads to the Δ_5–Δ_8 parameters [42]. Δ_9 is an interaction between the two anions in the unit cell, an effect which is missing for ZB.

A closer comparison is to the CC model. Recall that the latter is only described by three parameters, Δ_1–Δ_3 at $\mathbf{k} = \mathbf{0}$. This reflects some of the shortcomings of the CC model–even though the latter is widely used.

3.5 Summary

It was shown how perturbation theory can be used to obtain the valence-band Hamiltonian for both cubic and hexagonal crystals. The cubic case was done specifically for the Dresselhaus–Kip–Kittel Hamiltonian and the latter was related to a few other Hamiltonians in the literature. It was found that the DKK Hamiltonian, in the absence of spin-orbit coupling and an external magnetic field, only has three band parameters. The case of a wurtzite semiconductor was then treated along similar lines; for the most widely used valence-band model, the Hamiltonian has 10 band parameters. Variations on the latter model were then discussed.